Dissertation

THE ENDOCANNABINOID SYSTEM IN INTESTINAL INFLAMMATION AND COLON CANCER: ROLE OF G PROTEIN-COUPLED RECEPTOR 55 AND MONOACYLGLYCEROL LIPASE

submitted by

Angela Annamagdalena STANČIĆ

for the Academic Degree of
Doctor of Philosophy
(PhD)

at the
Medical University of Graz
Institute of Experimental and Clinical Pharmacology

under the Supervision of
Assoc. Prof. Rudolf Schicho

2015

Declaration of authenticity

I hereby declare that this dissertation is my own original work and that I have fully acknowledged by name all of those individuals and organizations that have contributed to the research for this dissertation. Due acknowledgement has been made in the text to all other material used. Throughout this dissertation and in all related publications I followed the guidelines of “Good Scientific Practice”.

Graz, July 2015

Aknowledgements

First and foremost I would like to thank Prof. Rudolf Schicho for giving me the opportunity to work under his supervision and for his patience, advice, guidance, and attention to detail throughout my research. He, more than any other, has contributed to my professional growth.

Special thanks also to Ing. Veronika Pommer, who together with Prof. Schicho taught me everything in the laboratory.

I am much obliged to the head of the Institute, Prof. Akos Heinemann, who has helped and advised me in many occasions, and to the whole Institute of Experimental and Clinical Pharmacology for all their help.

My sincere thanks go to Prof. Rufina Schuligoi and Prof. Gerald Höfler for agreeing to be part of my thesis committee, and for their invaluable help and advice.

At the end, I would like to thank Karin, Ivan, Nada and Zvonko for their infinite support.

“Hope is a good thing maybe the best of all things” – the Shawshank redemption

This work I dedicate to Bo and Gio

Table of contents

Abbreviations

2-AG – 2-arachidonoylglycerol

Δ^9-THC - Δ^9 tetrahydrocannabinol

AA – arachidonic acid

ABHD6 – abhydrolase domain-containing protein 6

ABHD12 – abhydrolase Domain Containing Protein 12

AOM – azoxymethane

APC – adenomatous polyposis coli

C5a – complement component 5a

CAC – colitis associated cancer

CB1 – cannabinoid receptor 1

CB2 – cannabinoid receptor 2

CBD – cannabidiol

CD – Crohn´s disease

CD3 – cluster of differentitation molecule 3

CD11b – cluster of differentiation molecule 11b

CMF – calcium and magnesium free

CO_2 – carbon dioxide

COX-1 – cyclooxygenase 1

COX-2 – cyclooxygenase 2

CRC – colorectal cancer

DAG – diacylglycerol

DAGL – diacylglycerol lipase

DMEM – Dulbecco´s modified eagle medium

DMSO – dimethylsulfoxid

DSI – depolarization-induced suppression of inhibition

DSS – dextrane sulfate sodium

EC – endocannabinoid system

ECs – endocannabinoids

EDTA – ethylenediaminetetraacetic acid

ELISA – enzyme linked immunosorbent assay

EMT – endocannabinoid membrane transporter

ERK – extracellular-signal-regulated kinase

FAAH – fatty acid amide hydrolase

FACS – fluorescence-activated cell sorting

FAS – fatty acid synthase

FBS – fetal bovine serum

f-MLP – Formyl-Methionyl-Leucyl-Phenylalanine

GI- gastrointestinal

GPCR – G protein-couples receptor

GPR55 – G protein-coupled receptor 55

HBSS – Hank´s balanced salt solution

HEPES - (4-(2-hydroxyethyl)-1-piperazineethanesulfonic acid)

HETE – hydroxyeicosatetraenoic acid

HPETE – hydroxyperoxyeicosatetraenoic acid

HTAB – Hexadecyltrimethylammonium bromide

H_2O_2 – hydrogen peroxide

IBD – inflammatory bowel disease

IFN-α – interferon α

IFN-γ – interferon γ

IL-1 – interleukin 1

IL-1β – interleukin 1β

IL-4 – interleukin 4

IL-6 – interleukin 6

IL-10 – interleukin 10

IL-11 – interleukin 11

IL-12 – interleukin 12

IL-13 – interleukin 13

IL-23 – interleukin 23

K_2HPO_4 – potassium phosphate, dibasic

KCl – potassium chloride

kDa - kilodalton

KH_2PO_4 – monopotassium phoshate

K-RAS - V-Ki-ras2 Kirsten rat sarcoma viral oncogene homolog

LPI – α-lysophosphatidylinositol

LPS – lipopolysaccharide

MAGL – monoacylglycerol lipase

MAPK – mitogen-activated protein kinase

MCP-1 – monocyte chemoattractant protein 1

MPO – myeloperoxidase

m-RNA – messenger ribonucleic acid

NaCl – sodium chloride

NAPE-PLD - N-acetylphosphatidylethanolamine-hydrolysing phospholipase D

NFAT – nuclear factor of activated T-cells

NFκB – nuclear factor kappa light chain enhancer of activated B cells

NKT – natural killer T cell

NSAID – nonsteroidal antiinflammatory drug

PBS – phosphate buffered saline

PDE3A – phosphodiesterase 3A

PDE4B – phosphodiesterase 4B

PI3K – phosphatidylinositol-3-kinases

PLC – phospholipase C

PS – penicillin-streptomcyin

pSTAT3 – phosphorylated signal transducer and activator of transcription 3

RT-PCR – reverse transcription polymerase chain reaction

SDS – sodium dodecyl sulfate

TGFβ – transforming growth factor β

Th2 – T- helper cell type 2

TNBS – 2,4,6 –trinitrobenzene sulfonic acid

TNF-α – tumor necrosis factor α

TNFR1 – tumor necrosis factor receptor 1

TNFR2 – tumor necrosis factor receptor 2

TRIS/HCL – (hydroxymethyl)aminomethane / hydrochloride

TRPV1 – transient receptor potential cation channel subfamily V member 1

TRPV4 – transient receptor potential cation channel subfamily C member 4

t-STAT3 – total signal transducer and activator of transcription 3

UC – ulcerative colitis

Summary

Endocannabinoids, such as anandamide and 2-arachidonoylglycerol (2-AG), are thought to play an important role in intestinal inflammation. They exert their actions via cannabinoid receptors 1 and 2 (CB1 and CB2) and probably via G protein-coupled receptor 55 (GPR55), which are part of the endocannabinoid system. Monoacylglycerol lipase (MAGL) is also part of the endocannabinoid system and is the key enzyme responsible for degrading 2-AG and is expressed not only in the brain, but also throughout the digestive tract.

GPR55 is an atypical cannabinoid receptor and has been shown to be implicated in several pathophysiologic functions. However, its main agonist is the phospholipid lysophosphatidylinositol (LPI), which is not a cannabinoid, but some endocannabinoids were shown to exert their actions also via the GPR55 receptor. $GPR55^{-/-}$ knockout mice have no evident phenotype but inhibition of GPR55 is thought to be protective in models of neuroinflammation.

Here, I investigated the effects of the MAGL inhibitor (JZL184) as well as a GPR55 antagonist (CID16020046) in mouse models of experimental colitis and colitis-associated cancer. In addition, I used $MAGL^{-/-}$ and $GPR55^{-/-}$ knockout mice.

The GPR55 antagonist was able to reduce the severity of dextrane sulphate sodium (DSS) and 2,4,6-trinitrobenzenesulfonic acid (TNBS) induced colitis, as well as to reduce leukocyte recruitment into the lamina propria of the colon. $GPR55^{-/-}$ mice were also protected from severe intestinal inflammation. Cytokine expression was reduced in the selective GPR55 antagonist treated group. Incubation of mouse macrophage cell line J774.1 with the GPR55 antagonist decreased C5a-induced migration and CD11b expression. Chemotaxis of human neutrophils was also inhibited by GPR55 antagonist treatment.

The MAGL inhibitor JZL184 decreased the extent of inflammation in the DSS-induced colitis at a high dose of 32mg/kg, as well as it reduced total tumor area in a model of colitis-driven colon cancer at a low dose. $MAGL^{-/-}$ mice had significantly less tumors and less severe intestinal inflammation compared to wild-type mice.

Unlike the cannabinoid receptors, GPR55 plays a proinflammatory role in experimental colitis, and genetic and pharmacological inhibition of MAGL improved the course of the colitis and may therefore represent interesting therapeutic targets for inflammatory bowel diseases.

Zusammenfassung

Endocannabinoide, wie z. B. Anandamid und 2-Arachidonylglycerol (2-AG), spielen eine wichtige Rolle bei der Darmentzündung. Sie wirken über Cannabinoid- (CB1 und CB2) und GPR55-Rezeptoren, die Teil des Endocannabinoid-Systems sind. Monoacylglycerol Lipase (MAGL) das Schlüsselenzym für den Abbau von 2-AG ist im Gehirn, und auch in dem gesamten Verdauungstrakt exprimiert.

GPR55 ist ein atypischer Cannabinoid-Rezeptor, der mit einigen pathophysiologischen Funktionen in Verbindung gebracht wird. Sein Agonist ist das Phospholipid Lysophosphatidylinositol (LPI), das selbst kein Cannabinoid ist. Dennoch wirken einige Cannabinoide auch über den GPR55-Rezeptor. GPR55$^{-/-}$ knockout Mäuse haben keinen offensichtlichen Phänotyp, aber in Modellen wurde gezeigt, dass die Inhibierung von GPR55 einen gewissen Schutz vor neuropathischen und entzündungsbedingten Schmerzen bewirkt.

In meiner Doktorarbeit untersuchte ich die Auswirkungen des MAGL Inhibitors JZL184 sowie des GPR55-Antagonisten CID16020046 in Modellen von experimenteller Kolitis und Kolitis-assoziiertem Krebs in Mäusen.

Der GPR55-Antagonist konnte das Ausmaß der chemisch-induzierten experimentellen Kolitis verringern, sowie auch die Leukozytenrekrutierung in die Lamina propria des Kolons verringern. GPR55$^{-/-}$ knockout Mäuse waren vor einer schweren Darmentzündung geschützt. Die Zytokin-Expression war in der mit dem selektiven GPR55 Antagonisten behandelten Gruppe reduziert. Die Inkubation der Maus-Makrophagen-Zelllinie J774.1 mit dem GPR55-Antagonist verringerte C5a-induzierte Migration und die CD11b-Expression. Die Chemotaxis von humanen Neutrophilen wurde durch den GPR55-Antagonisten gehemmt.

Der selektive Inhibitor von MAGL, JZL184, verringerte das Ausmaß der Entzündung in der experimentellen Kolitis, sowie auch die Gesamtfläche der Tumore in einem Modell von Kolitis-induziertem Darmkrebs. MAGL $^{-/-}$ knockout

Mäuse hatten signifikant weniger Tumore und weniger schwere Darmentzündung im Vergleich zu Wildtyp-Mäusen.

Im Gegensatz zu den Cannabinoidrezeptoren spielt GPR55 eine proinflammatorische Rolle in der experimentellen Kolitis. Genetische und pharmakologische Hemmung der MAGL verbessert den Verlauf der Erkrankung. Somit stellen diese Bestandteile des Endocannabinoid-Systems interessante therapeutische Ziele für entzündliche Darmerkrankungen da.

1. Introduction

1.1. Role of endocannabinoid system in inflammation and colon cancer

Cannabis has been traditionally used to alleviate symptoms in a variety of diseases and in many inflammatory conditions, such as neuroinflammation and gastrointestinal diseases. How cannabinoids may provide a benefit to people with intestinal inflammation, such as inflammatory bowel disease and neoplasm of the bowel is largely unknown. My thesis, therefore, focused on the role of the endocannabinoid system, specifically on two of its components, i.e. GPR55 and 2-AG, in the pathophysiology of inflammatory bowel disease and colitis-associated colon cancer.

1.2. Inflammatory bowel disease

Inflammatory bowel disease (IBD) in humans is a chronic relapsing and remitting inflammatory condition of the gastrointestinal tract without yet known origin of the disease (1,2). Two major forms of IBD are Crohn's disease (CD) and ulcerative colitis (UC) with an incidence of 0,15-0,2% of the western population (3).

Crohn's disease affects the whole alimentary tract, but most frequently the transmural granulomatous inflammation occurs in the terminal ileum and ascending colon (4). Since all layers of the digestive tract may be affected, fissures and fistula occur as a severe complication (5). The main characteristic of UC is, distinct to the pathophysiology of CD, a superficial inflammation of the mucosa causing disruption of crypt morphology and depletion of goblet cells which leads to ulcers (6). The disease is prevalently centered in the rectum and colon (4). Crohn's disease is associated with a Th1-cell-mediated immune response

induced by interleukin-12 (IL-12), tumor necrosis factor α (TNF-α), interferon α (IFN-α) and possibly interleukin-23 (IL-23). UC is characterized with a Th2 type T-cell-mediated response, mediated by interleukin-13 (IL-13) secreted by natural killer T (NKT) cells (4,7).

A mutual role of genetic and environmental factors has been suggested to be the cause of IBD diseases (8,9). Up to 40% of first grade relatives might also develop IBD throughout life (10). Environmental factors that might have an implication on the development of IBD include childhood infections, oral contraceptives, diet, hygiene, education, occupation, pollution, appendectomy, tonsillectomy, contact with animals and physical activity (10). Various studies have suggested a dysregulated, excessive and prolonged mucosal response to unknown antigens present in the normal bacterial microflora (4,8,11,12) . This dysregulated response might have its cause in genetic factors, which in turn are activated by environmental factors. Some of these environmental factors might be those that influence the composition of the bacterial microflora of the gut itself (8). In addition, an imbalance between proinflammatory (TNF-α, interferon-γ (IFN-γ), IL-1, IL-6, IL-12) and antiinflammatory (IL-4, IL-10, IL-11) mediators (e.g. cytokines) has been suggested to play an important role in the development of UC and CD (13).

Up to date, the main therapy of IBD is based on symptom-relieving treatments by using aminosalicylates (5-amino salicylic acid derivatives) and glucocorticoids. Other treatment possibilities include the use of immunosuppressive drugs such as azathioprine, 6-mercaptopurine, methotrexate and cyclosporine. However, use of all those medications is accompanied by serious side effects, like acute pancreatitis, abdominal pain, diarrhea, nausea and headache after 5-amino salicylic acid-based agents or Cushing´s syndrome after glucocorticoid treatment (14). Because of the traditional knowledge that Cannabis may ameliorate symptoms of IBD and because of a recent trial which showed that Cannabis consumption may be helpful in alleviating abdominal pain, loss of appetite, nausea and diarrhea via cannabinoid and possibly other receptors, cannabinoids and

drugs that modulate the endocannabinoid system might be an interesting possible target for treating inflammatory bowel diseases (15–17).

1.3. Inflammation and colon cancer

Patients with IBD have a significantly higher risk of developing colorectal cancer than people with no IBD. Almost 50% of people with colitis-associated colorectal cancer (CAC) will die within 30 years of disease onset (18). With about 5% of the adult population being affected with CAC, it is one of the very common fatal malignancies worldwide. During permanent colonic inflammation, reactive oxygen and nitrogen species are produced that cause DNA damage and possibly alter cell proliferation and survival, which then promotes oncogenesis (19). Interestingly, chronic inflammation is being suggested as a tumor promoter rather than a tumor initiator (20). It is suggested that immune cells that infiltrate preneoplastic lesions and/or tumors produce cytokines and chemokines that, next to a localized inflammatory response, boost the growth and survival of premalignant cells, as for instance by activating nuclear factor kappa-light-chain-enhancer of activated B cells (NFκB) (19). Colorectal cancer (CRC) and colitis-associated colorectal cancer (CAC) have the main and essential stages of cancer development in common (18). However, injury-dysplasia (develops without formation of a well-defined adenoma) and chronic inflammation is characteristic only of CAC. Proteins such as β-catenin, K-ras, p53, transforming growth factor β (TGFβ) are upregulated in both colorectal cancer forms (21). Interestingly, inflammation without repeating cycles of injury and repair is not enough for tumor development (18).

1.4. Cannabinoids and colon cancer

Cannabinoids were successfully used for centuries as a treatment against pain, depression, lack of appetite and inflammation as well as a relief for cancer patients

by alleviating nausea and vomiting caused by chemotherapy (22). Today, cannabinoid receptor agonists are used for the treatment of anorexia, pain, spasticity and emesis (23). The first indication that cannabinoids possibly have antitumorigenic effects was in 1975, when the growth of Lewis lung adenocarcinoma was inhibited after Δ^9-tetrahydrocannabinol (Δ^9-THC) and cannabinol treatment *in vitro*, as well as after oral administration to the mice. In following studies, antiproliferative, antimetastatic, antiangiogenic and proapoptotic effects of cannabinoids were shown (24,25). These observations on effects of cannabinoids (endogenous, plant-derived and synthetic analogues) were studied both *in vitro* and *in vivo* in various cancer types, for instance prostate, breast, pancreas, skin, lymphoma, thyroid, and lung cancer (22,26).

1.5. The endocannabinoid system and its components

The endocannabinoid system (EC) is defined as a system consisting of two G-protein-coupled receptors (GPCRs), called cannabinoid receptors 1 and 2 (CB1 and CB2); two representative endogenous lipid ligands, N-arachidonoylethanolamine (anandamide) and 2-arachidonoylglycerol (2-AG); as well as the endocannabinoid biosynthetic (N-acyl phosphatidylethanolamine phospholipase D (NAPE-PLD) and diacylglycerol lipase (DAGL)) and catabolic enzymes (MAGL and FAAH) (27–29). GPR55 and transient receptor potential cation channel subfamily V member 1 (TRPV1), two receptors responsive to endocannabinoids, can be considered part of an extended EC (16) (Figure 1). The EC system is involved in the pathophysiology of several diseases such as obesity, osteoporosis, neuropathic and inflammatory pain, cardiovascular disorders and liver disease (30).

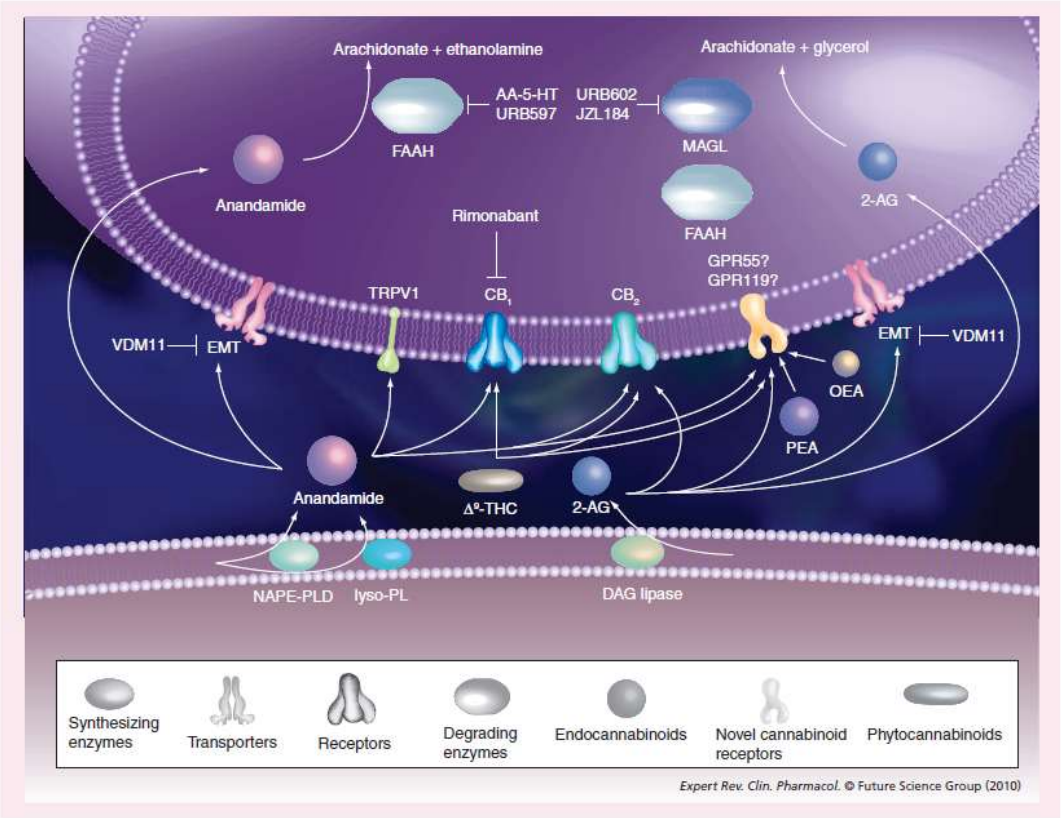

Figure 1

The endocannabinoid system. Synthesis of endocannabinoids involves several steps using membrane phospholipids as substrates. NAPE-PLD and lyso-PLD catalyze the final reaction in the production of anandamide. DAG lipase uses diacylglycerols as substrates to produce 2-AG. After diffusion into the extracellular space, anandamide and 2-AG bind to CB1 and CB2, to TRPV1 and to a potentially novel CB receptor, such as GPR55. Their action is terminated by cellular reuptake via the endocannabinoid membrane transporter (EMT) or by passive diffusion. Anandamide is subsequently degraded by fatty acid amide hydrolase and 2-AG by monoacylglycerol-lipase and FAAH, respectively. Picture taken from (31).

CB1 receptors are expressed mainly in the brain, but also in other tissues, as for instance spleen, testis, adipose tissue and the gastrointestinal tract, whilst the highest density of CB2 receptors is mainly found in cells and organs of the immune system (22,32). The density of CB1 receptor expression in the brain is up to 50-fold higher than of other GPCRs, such as dopamine and opioid receptors. This makes it the most abundant GPCR in the brain (29). However, both cannabinoid receptors are also expressed in the enteric nervous system,

particularly on nerve fibers and terminals of cholinergic enteric neurons (24,33). In experiments with intestines from mice, rats and guinea pigs, cannabinoids reduced electrically-induced contractions of the colon mainly via CB1 receptor activation, indicating a possibility for cannabinoids to reduce hypermotility of an inflamed colon (24,34). Activation of the CB1 receptor increases food intake, inhibits vomiting and gastric fundus contractions, as well as contractions of the ileum and colon, and slows down the colonic transit (31). The inverse agonist of the CB1 receptor, rimonabant, was clinically introduced as an effective weight loss agent (Acomplia®), but was withdrawn in October 2008 from the European market because of its side effects like increased depression (35). In several models of neuropathic pain and inflammation, cannabinoid receptor agonists exert antinociceptive and antiinflammatory actions (23).

CB1 activation stimulates cellular signal transduction via $G_{i/o}$, but CB2 couples strongly to G_i. CB receptor activation causes inhibition of adenylate cyclase, and activation of the mitogen-activated protein kinases (MAPKs) and phosphoinositide 3-kinase (PI3K) thereby regulating many complex signaling pathways that for instance influence cell death (apoptosis) and cell proliferation (36,37). Several human colorectal cancer cell lines undergo apoptosis after treatment with cannabinoids that act via CB1 receptors (38,39). CB1 receptors can also modulate ion channels, thus inhibiting N-, and P/R-type calcium channels, stimulating inwardly rectifying potassium channels and enhancing the activation of A-type potassium channels (40,41).

1.6. The atypical cannabinoid receptor GPR55

In many studies, various effects of exogenous and endogenous cannabinoids could not be explained by activation of CB1 or CB2 (42). Therefore, it has been suggested that GPR55, which is responsive to certain cannabinoids, might represent another cannabinoid receptor. But so far, this theory could not be proven (43,44) since the only true endogenous ligand for GPR55 is the phospholipid L-α-

lysophosphatidylinositol (LPI), and the only cannabinoids that exert real affinity towards the GPR55 are synthetic (61,62). GPR55 was the first time isolated and cloned in 1999 (45). It is a phospholipid receptor that is expressed in the bone marrow, spleen, immune cells, endothelial cells, central nervous system, vasculature, placenta and throughout the intestine (duodenum, jejunum, ileum and colon) and is also found in cancer tissues and cancer cell lines (29,45–47) (Figure 2). Particularly for the gastrointestinal tract, it was shown that GPR55 was expressed in mucosal scrapings and in longitudinal-myenteric plexus preparations (48).

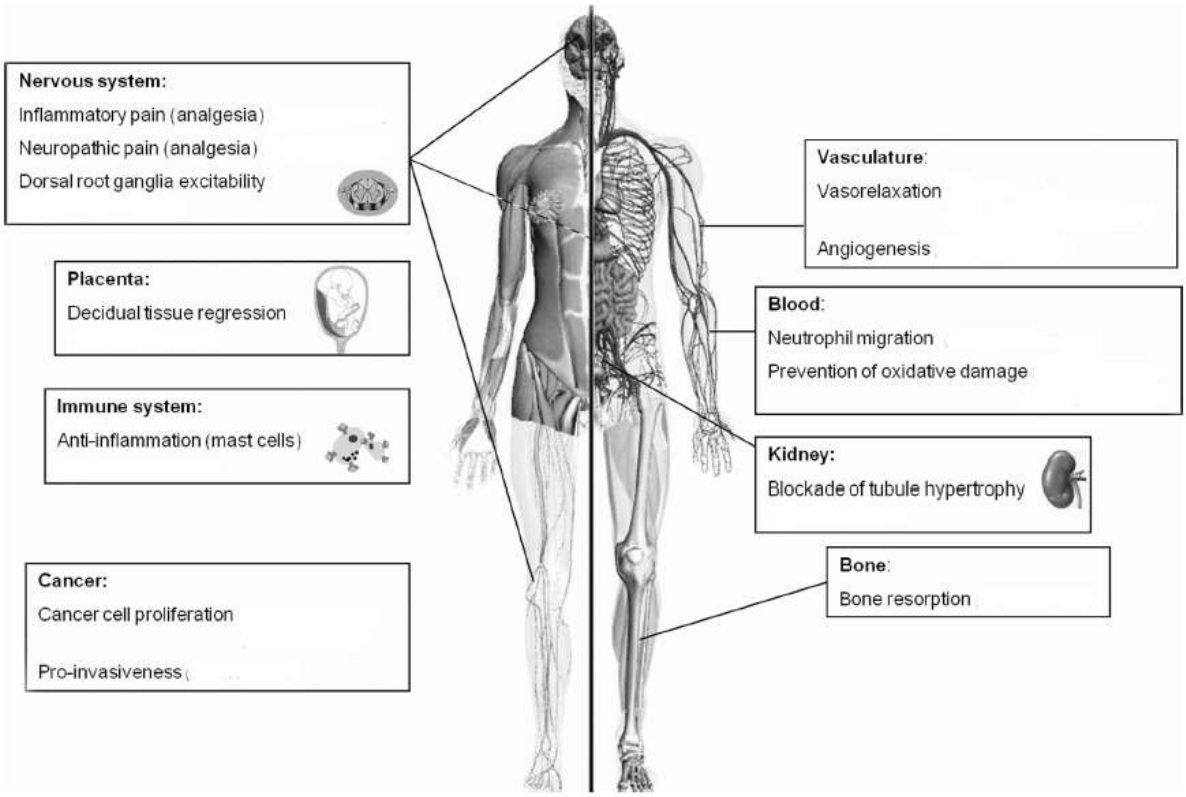

Figure 2

GPR55 is widely expressed in various organs as well as in the immune system, and also has an important role in carcinogenesis. Picture taken from (46).

GPR55 has a 13% homology with the CB1 receptor and 14% with the CB2 receptor (45). The biggest similarity GPR55 has with other receptors is the purinergic receptor P2Y5 (44). In contrast to CB1 and CB2 receptors, GPR55 signals through $G\alpha_{12/13}$ G protein and not through $G_{i/o}$ (49). GPR55 initiates excitatory effects, whilst CB1 and CB2 initiate more inhibitory effects (48). Activation of GPR55 results in ERK phosphorylation and an increase in intracellular Ca^{2+} (Figure 3) (30,50). It has also been shown that upon GPR55 activation, nuclear factor of activated T-cells (NFAT), nuclear factor k-light chain-enhancer of activated B cells (NFκB), and MAP kinases (p38 and ERK 1/2 MAPK) are activated (51,52). Due to the fact that LPI alone is able to significantly activate ERK1/2, but endocannabinoids (anandamide and 2-AG) caused little or no response, it has been suggested that cannabinoids and LPI display functional selectivity (42). GPR55 does not possess the typical "cannabinoid binding pocket", but has a rather deep, vertical and highly hydrophilic binding pocket in its active conformation, and in addition a longer third extracellular loop (53). Recently, it was shown that herbal cannabinoids like Δ^9-tetrahydrocannabivarin, cannabidivarin, and cannabigerovarin were able to non-competitively inhibit the actions of LPI on GPR55 (54). Since those cannabinoids acted as agonists when applied alone, it was suggested that GPR55 possesses an orthosteric and an allosteric binding site (50) (Figure 4).

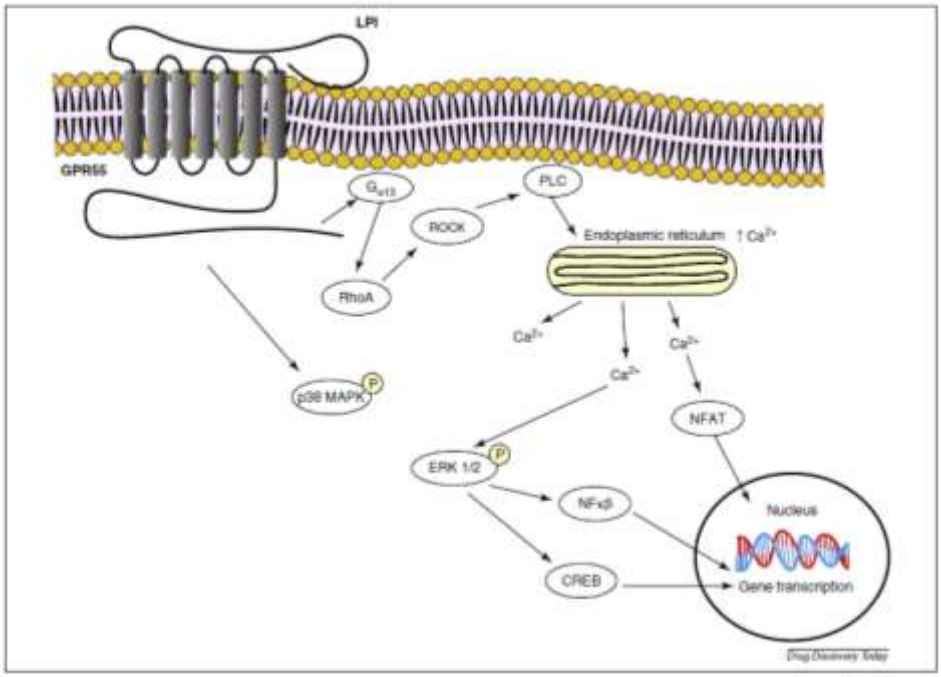

Figure 3

Downstream signaling pathways of GPR55 activation by LPI in human embryonic kidney (HEK293) cell overexpressing GPR55. Activation of Gα13 triggers Ras homologue gene family member A (RhoA)-dependent release of oscillatory calcium from the endoplasmic reticulum (ER), which then further results in extracellular signal-regulated kinase 1/2 (ERK1/2) phosphorylation. Nuclear factor kappa light polypeptide gene (NFkB) enhances B cells and 30–50-cyclic adenosine monophosphate response binding protein (CREB) activation. Elevated calcium release by the ER activates nuclear factor of activated T cells (NFAT), which causes translocation from the cytosol to the nucleus. GPR55 activation by LPI also causes p38 mitogen activated protein kinase (p38 MAPK) phosphorylation. Picture taken from (55)

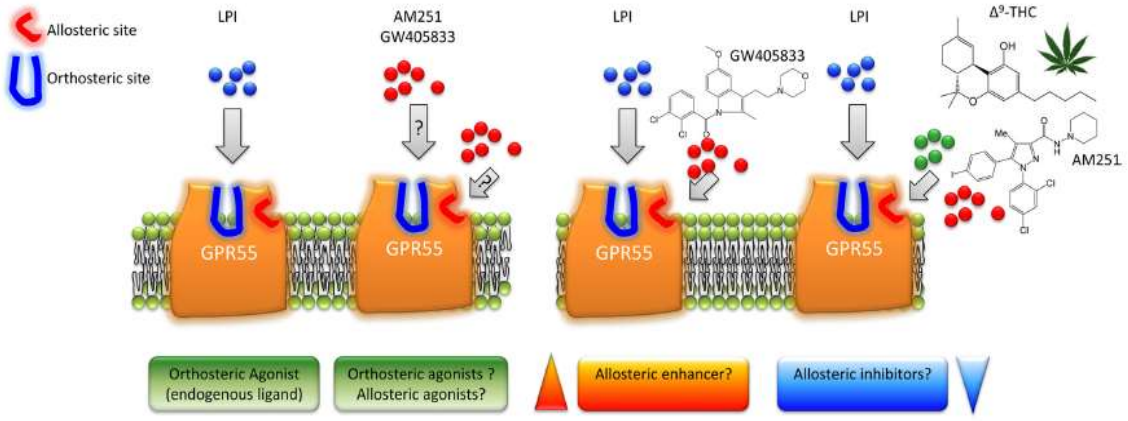

Figure 4

LPI is suggested to primarily bind the GPR55 orthosteric binding site. GPR55 may also contain an allosteric binding site. These observations raise at least two possibilities as follows: left, one possibility is that certain arylpyrazole ligands actually represent bitopic ligands of GPR55. These ligands may have the capacity to modulate both the orthosteric (agonists) and the allosteric site through different pharmacophores. The second possibility is that AM251 and certain arylpyrazole analogues are only allosteric ligands. Right, in the presence of LPI, arylpyrazoles can also behave as allosteric inhibitors and GW405833 as an allosteric enhancer. In addition, a number of *Cannabis sativa* constituents appear to inhibit ERK1/2 phosphorylation in an allosteric manner. Picture taken from (54).

Inhibition of GPR55 signaling was shown to reduce inflammation and neuropathic pain (56). In lipopolysaccharide (LPS) - induced experimental gastrointestinal (GI) inflammation, cannabidiol (a cannabinoid acting as a GPR55 antagonist) was shown to have a protective effect via reduction of proinflammatory cytokine production, inhibition of neutrophil infiltration and prevention of tissue damage (57). Also, LPS treatment caused higher GPR55 expression compared to the control group (57). One year later, the protective effect of cannabidiol (CBD) was shown in murine intestinal inflammation by intrarectal application (58). The interesting fact about this study was that it was shown that even topically and not only systemically applied CBD was protective against gastrointestinal damage (58). A possible, albeit unspecific, agonist of GPR55, O-1602, is a synthetic cannabidiol analogue and is protective in murine colitis models (49). It is inactive on CB1 and CB2, and also shows GPR55 independent effects (49). It has been

suggested that GPR55 has a higher impact on gut motility in pathological conditions like inflammation than in healthy physiological conditions (48).

GPR55 has been shown to form heteromers with both cannabinoid receptors (51,59). CB1-GPR55 heteromers were shown in HEK293 cells that overexpressed both receptors (51). GPR55 signaling was inhibited when the CB1 receptors were also inhibited, whilst this was not the case vice versa (51). On the contrary, CB1 receptor signaling is enhanced in the presence of GPR55 receptors. When CB1 receptors are activated, GPR55 signaling is restored (51). CB2-GPR55 heteromers were recently shown in cancer cells, where they have a major impact on the cannabinoid signaling in these cells (60). Also, when both the CB2 and GPR55 were activated on human neutrophils, chemotaxis was significantly enhanced at the level of downstream signaling molecules, such as RhoA (47). However, the heteromers seem to loosen after the initial functional synergism and then GPR55 inhibits downstream signaling of CB2.

Recently, a promising selective GPR55 antagonist was described, CID16020046 (61). A big advantage of CID16020046 versus cannabidiol, is that it is inactive on the TRPV4 channel, and that it is selective for GPR55 over CB1. The biggest impact CID16020046 had outside GPR55 was on the phosphodiesterases PDE3A and PDE4B. ERK 1/2 phosphorylation by LPI was successfully blocked with CID16020046, but CID16020046 did not have any effect on CB1/CB2-mediated ERK 1/2 phosphorylation. Also, pretreatment with CID16020046 inhibited GPR55 internalization (61). $GPR55^{-/-}$ knockout mice are protected in models of neuroinflammation, but have no different phenotype to the wild type mice (56).

1.7. The main endocannabinoids: anandamide and 2-AG

Of the endogenous ligands of the CB receptors, the first of them, anandamide, was described in 1992 (62). The ECs were discovered in studies that were trying to elucidate the molecular mechanism of Δ^9-THC, the main psychotropic

compound of the *Cannabis sativa* plant (63). Two of the main ECs, 2-AG and anandamide are derivatives of arachidonic acid, a n-6 polyunsaturated fatty acid (28,64). Both of the ECs, unlike classical neurotransmitters, are synthesized and released on demand by remodeling of membrane lipids, depending on different pathological and physiological stimuli (30,37,65). They enter the intercellular space, where they bind their receptors and then get inactivated by facilitated diffusion via protein transporters (62,66). If the concentration of the endocannabinoids is higher in the extracellular than in the intracellular space, they probably can also diffuse though the plasma membrane, since they are lipophilic in nature (29,67). Anandamide is a partial agonist of both cannabinoid receptors with an approximately fourfold higher affinity to CB1 than to CB2 (27,28). It is produced by cleavage of N-arachidonoyl-phosphathidylethanolamine (NAPE). The main enzyme responsible for anandamide (and other N-acyl-ethanolamines) degradation is fatty acid amide hydrolase (FAAH), a membrane-bound hydrolase enzyme that has been found co-localized with the CB1 receptor in the brain of rats (66). 2-AG is a full agonist on both the cannabinoid receptors, and its content in mouse brain, ileum and colon tissues is a few orders of magnitude higher than that of anandamide. 2-AG may also inhibit the cellular uptake of anandamide (67–69). In the digestive tract, 2-AG has a higher expression in the ileum than in the colon, whilst anandamide has higher expression levels in the colon than in the ileum, although a recent report finds that in MAGL knockout mice the 2-AG content is higher in the colon than in the duodenum, jejunum, and ileum respectively (70,71). In the brain, it is released from postsynaptic neurons and mediates retrograde synaptic suppression through CB1 receptors found on presynaptic terminals (Figure 5) (28,65). Hydrolysis of membrane phospholipids by phospholipase C (PLC) produces 1,2-diacylglycerol, which is then hydrolyzed to 2-AG by the action of diacylglycerol lipase (DAGL) (64). 2-AG has been shown to have many beneficial properties, such as analgesic, antiinflammatory, neuroprotective and hypotensive effects, as well as an important role in the regulation of the innate and adaptive immune system (72). Although FAAH is also able to degrade 2-AG into glycerol and arachidonic acid, this seems physiologically not relevant as brain 2-AG levels remain unaltered after either pharmacological or genetic inhibition of

FAAH (73). The main enzyme responsible for degrading 2-AG is monoacylglycerol lipase (MAGL), a 33kDa cytosolic serine hydrolase that completes the hydrolysis of metabolites of the lipoprotein lipase and the hormone-sensitive lipase (66,73,74).

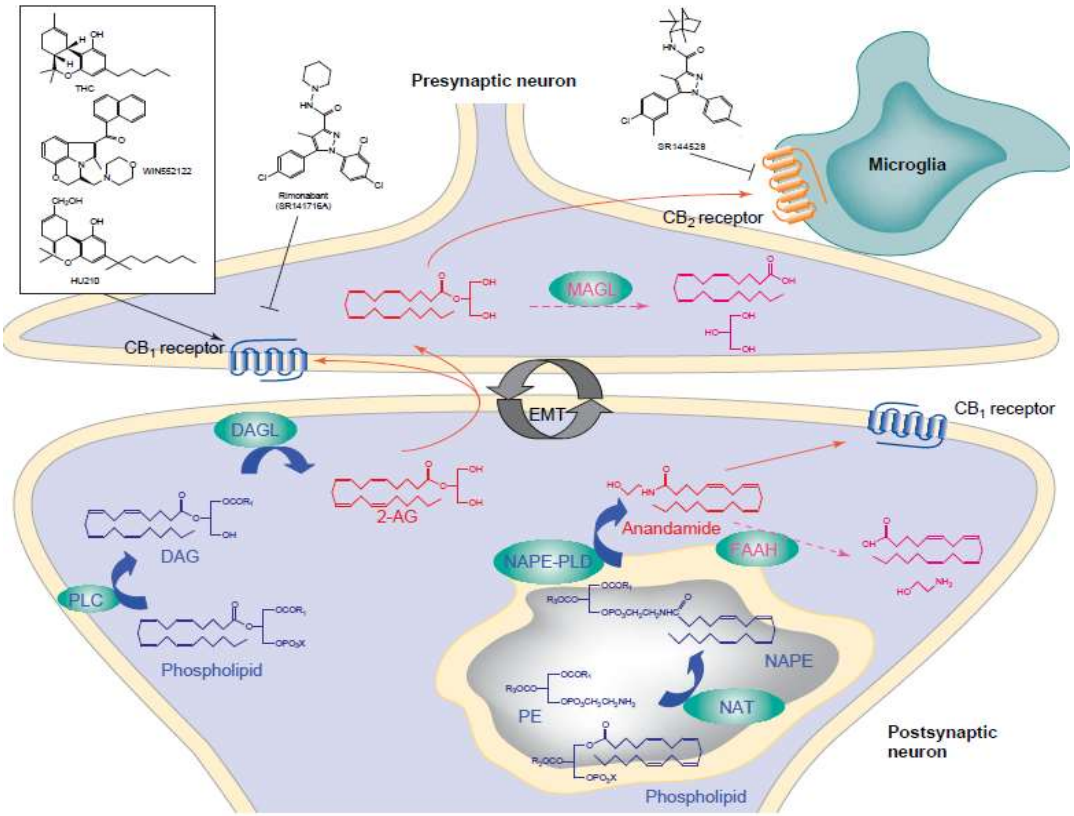

Figure 5 Cannabioid receptors are located on the presynaptic neuron, whilst 2-AG and anandamide are synthesized in the postsynaptic neuron acting as retrograde messengers. Picture taken from (65).

1.8. Monoacylglycerol lipase (MAGL) - the main producer of 2-AG

MAGL has been extensively studied in the brain, where it was shown to co-localize with CB1 receptors on presynaptic neurons, but it was not until recently, that MAGL was also identified in the gastrointestinal tract, (33,69,75). However, MAGL is also expressed in other peripheral tissues, such as in ovary, adrenal gland,

adipose tissue, heard and the kidney. In the brain, MAGL is responsible for up to 85% of 2-AG hydrolysis. The remaining 15% are hydrolyzed by α/β hydrolase domain 6 (ABHD6) and ABDH12 (76). Since 2-AG and anandamide are retrograde signaling molecules, a presynaptical localization of their main degrading enzymes seems logical but interestingly in rat hippocampus, cerebellum and amygdala, FAAH was found to be localized postsynaptically and MAGL presynaptically (75). It was shown that anandamide had no effect on the depolarization-induced suppression of inhibition (DSI) by using a selective FAAH inhibitor URB597 (77). MAGL is a biological dimer, a part of the α/β hydrolases superfamily. Six α helices surround the central β sheet consisting of seven parallel and one antiparallel strand. Below the cap domain that covers the active site a catalytic triad is placed made of three residues, Ser 112, Asp239 and His 269. The lipophylic and apolar residues of the α4 helix point to the outside of the protein, indicating that MAGL is present as an amphitopic enzyme in the cell, with an hydrophobic helix that allows the protein to get in close contact to the membrane and thereby offering an optimal entry for the voluminous hydrophobic substrate 2-AG (78).

In addition to 2-AG inactivation, it is thought that MAGL also produces a large pool of arachidonic acid, a precursor of eicosanoids (prostaglandins, tromboxanes, lipoxins, leukotrienes), making it an important link between endocannabinoid and eicosanoid signaling (23,64,79). Thus, arachidonic acid that originates from 2-AG breakdown could enter three different pathways; the cyclooxygenase pathway (generating mostly prostaglandins), the lipoxygenase pathway (generating mostly leukotrienes) and the P450 pathway (generating mostly hydroxyeicosatetraenoic acids (HETEs) and hydroxyperoxyeicosatetreanoic acids (HPETEs)) (80). In this context, it was discovered that patients with UC (and later, patients with CD as well) had significantly elevated levels of prostaglandins in mucosa tissue. Later it was shown that also tromboxanes, prostacyclines and leukotriene B4 were elevated in mucosal tissue of UC and CD patients. Interestingly, the use of nonsteroidal anti-inflammatory drugs (NSAID) to lower prostaglandin levels was of no benefit to IBD patients, and symptoms were rather worsened by their use

(10,81) suggesting a source other than Cox-2, possibly MAGL, for prostanoid production.

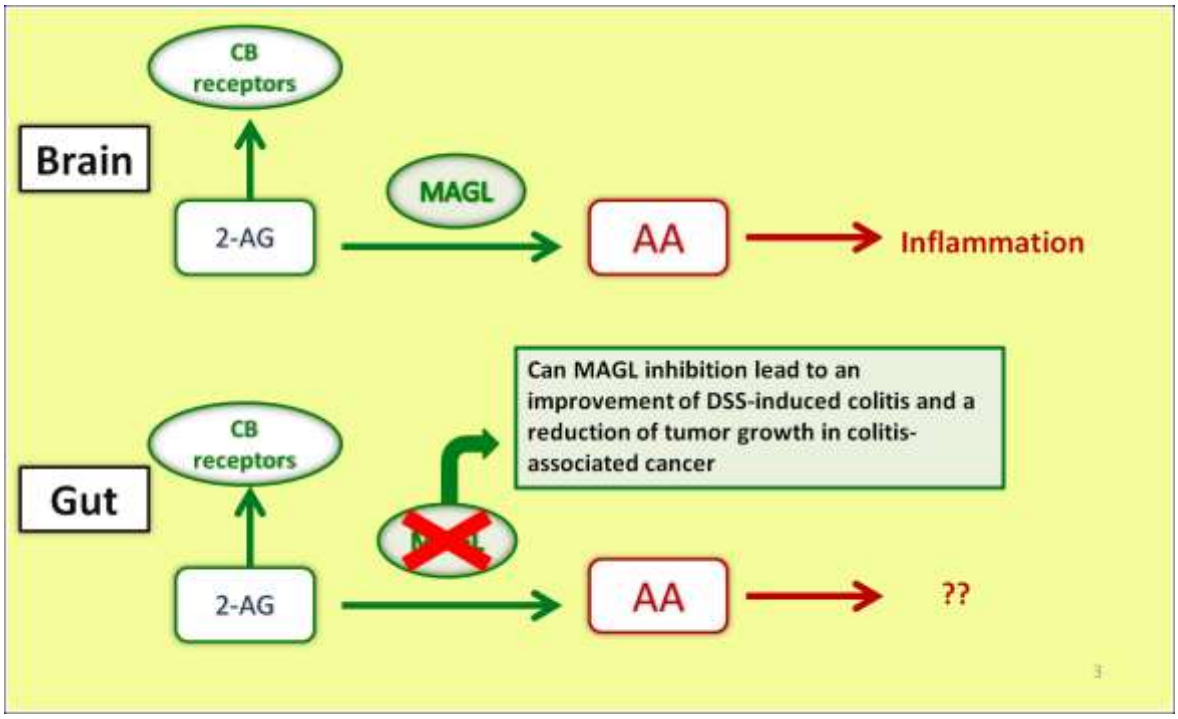

Figure 6

MAGL has been shown to be the main enzyme responsible for degrading 2-AG in the brain, leading to an increased pool of arachidonic acid, which is a precursor for inflammatory mediators. I hypothesized that MAGL inhibition could lead to a decreased inflammation in models of experimental colitis

Because the breakdown of 2-AG could feed an arachidonic acid pool from which many proinflammatory mediators may arise, (Figure 6). I hypothesized that inhibition of MAGL could improve intestinal inflammation. To investigate this, a MAGL inhibitor, JZL184, a substance that modifies the serine nucleophile of MAGL by covalent carbamylation, was used. JZL184 is a potent irreversible MAGL inhibitor that has been shown to significantly elevate 2-AG levels in the brain whilst anandamide levels were not affected (28,82). JZL184 treatment has been shown

to have CB1-dependent anti-allodynic and anti-edematous effects, and offered protection against gastric hemorrhages in mice caused by diclofenac treatment (27,83). Genetic or pharmacological (JZL184) inhibition of MAGL also showed tumor growth inhibition in xenograft models of melanoma, ovarian and colorectal cancer (84). A possible consequence of MAGL inhibition in ovarian cancer and melanoma may be the reduction of free fatty acid formation from various glycerol esters that are missing for the synthesis of oncogenic signaling lipids that promote cancer aggressiveness (23,85). In addition, inhibition of MAGL has been shown to affect general neurological functions, such as locomotor activity. These effects are not observed when FAAH is inhibited (83). Finally, inhibition of MAGL led to a lower bulk of arachidonic acid levels in the brain, and also reduced COX1-driven prostaglandin and thromboxane production in the brain (86).

1.9. Cannabinoids in inflammation and gastrointestinal cancer

The role of the CB receptors in intestinal inflammation has been extensively studied, and it was suggested that they play a protective role in inflammation by modulating the inflammatory response in the colon (87). Both cannabinoid receptors are expressed on natural killer cells, B cell and mast cells that are involved in the immune response of the gut (88). However, immune cells appear to be more modulated by CB2 receptor activation (89). Upon stimulation with lipopolysaccharide (LPS), macrophages, dendritic cells and mononuclear cells produce endocannabinoids (90). Genetic CB1 receptor depletion or pharmacological inhibition by the specific CB1 antagonist SR141716A made mice more susceptible to inflammation, indicating a protective role of CB1 during intestinal inflammation (87,91) and cannabinoids were shown to act via CB1 to promote epithelial wound healing (88,92). In a model of cholera toxin-induced intestinal hypersecretion, CB1 receptors were shown to be overexpressed, and exogenously administered anandamide had an protective effect on cholera toxin-induced fluid accumulation (93). Like already mentioned, the endocannabinoid system has a great impact on food intake and body weight regulation. Elevated

levels of anandamide and 2-AG are closely correlated with intra-abdominal adiposity (94). Mice lacking the CB1 receptor are resistant to diet-induced obesity (95). Combining those two facts, fasted rats have been shown to have low CB1 expression, but in fed rats, the expression was increased again (96).

The endocannabinoid system influences cancer development of the digestive tract in many ways, but mostly anticarcinogenic effect have been described for cannabinoids by mechanisms such as autophagy, apoptosis and cell cycle arrest (97) In colorectal cancer, cannabinoids have shown antiproliferative effects in tumor cells (24,98). The human colorectal cancer cell lines SW480, HCT 116, Caco-2 and several others underwent apoptosis after activation of CB1 by cannabinoids (99). In cholangiocarcinoma cancer, 2-AG and anandamide have shown differential effects on tumor progression. Whilst anandamide had antiproliferative and proapoptotic effects, 2-AG caused proliferation on cholangiocarcinoma cell growth. Both mechanisms of action were receptor-independent. The authors suggested disruption of the lipid raft structure and subsequent disturbance of cell signaling cascades upon 2-AG application (26).

In my thesis I investigated the role of 2-AG in models of experimental colitis and colitis-associated colon cancer using MAGL knockout mice and pharmacological inhibition of MAGL. I further investigated the role of GPR55 in experimental models of colitis by use of a selective GPR55 antagonist and GPR55 knockout mice.

2. Materials and Methods

2.1. Mouse models

2.1.1. DSS-induced colitis

In order to induce colitis, male C57BL6/N mice (5-6 weeks old, 20-22g; Charles River, Sulzfeld, Germany) received 2.5% dextran sulfate sodium (DSS) (MP Biomedicals, Santa Ana, California, USA) supplemented in their drinking water *ad libitum* for a period of 5 days (48). DSS colitis is a standard model with many similarities of human ulcerative colitis (6,100,101). The recently characterized GPR55 antagonist, CID16020046 ((61), MolPort, Riga, Latvia) or vehicle was administered s.c. for 7 days (20 mg/kg). On the first day of the experiment, CID16020046 was injected 30 minutes before the exposure to DSS. The changes in the weight of the mice were monitored daily during 8 days. In a different set of experiments, JZL184 (Cayman Chemical, Ann Arbor, Michigan, USA) was injected s.c. to inhibit MAGL activity and applied once or twice daily at the dosage of 16 mg/kg (27). $GPR55^{-/-}$ (Mutant Mouse Regional Resource centers, North Carolina, USA) and $MAGL^{-/-}$ knockout mice (102) were exposed to DSS, without any pharmacological treatment. The mice were sacrificed on the 8^{th} day of the experiment by cervical dislocation under isoflurane anesthesia. The colon was macroscopically evaluated as recently described (49). Upon completion of the scoring, parts of the colon were immediately snap-frozen in liquid nitrogen while other parts were processed for histology.

2.1.2. TNBS-induced colitis

To investigate a model which more resembles Crohn´s disease than ulcerative colitis (8,103), 2,4,6-trinitrobenzene sulfonic acid (TNBS; Sigma) was applied to

mice as previously described (49,104). C57BL6/N mice received once intrarectally (i.r.) 4 mg of TNBS dissolved in 30% ethanol. Mice were lightly anesthetized with isoflurane before given TNBS i.r. by a gavage needle with a blunt end. Mice were weighed on the consecutive 2 days, and sacrificed on the 4th day of the experiment. The GPR55 antagonist, CID16020046 was administered for three days once daily at the dosage of 20 mg/kg s.c. On the first day, CID16020046 was injected half an hour before the TNBS administration. Upon completion of macroscopic scoring (49), some parts of the colon were immediately snap-frozen in liquid nitrogen while other parts were processed for histology.

2.1.3. Colitis-induced colon cancer

To study a potential inhibiting effect of the MAGL inhibitor JZL 184 on tumor growth in the colon, a model of colitis-induced colon cancer was conducted on male CD1 mice (4-5 weeks old; 20-22g; Charles River, Sulzfeld, Germany), which consisted of an intraperitoneal (i.p.) injection of the carcinogen azoxymethane (Sigma) (10mg/kg), after which the mice were given one week of rest followed by a 7 days exposure to DSS (2%) in their drinking water. After DSS exposure, three different time points of JZL 184 administration or vehicle (s.c.) were chosen. The time points were chosen after DSS application in order not to interfere with induction of inflammation.

1. The first group was treated right away after the DSS exposure (only 3 days in between). Mice were administered 16 or 32mg/kg of the MAGL inhibitor JZL 184 or vehicle for 15 consecutive days. Mice were sacrificed 9 weeks after DSS exposure.
2. The second time point was at the beginning of the 4th week after DSS exposure, at the dosage of 8mg/kg JZL 184 or vehicle for 15 consecutive days. Mice were sacrificed 7 weeks after DSS exposure.
3. The third time point was at the beginning of the 6th week after DSS exposure, at the dosage of 8mg/kg JZL 184 or vehicle for 15 consecutive days. Mice were sacrificed 8 weeks after DSS exposure.

The colon was evaluated under a dissection microscope (Olympus, Vienna, Austria). Tumor number and tumor area of single tumors was measured using electronic caliper #1112-150 (INSIZE, Germany). For each colon, the sum of all single tumor areas was calculated. Samples for PCR, Western Blot, lipid extractions and histology were taken. Male $MAGL^{-/-}$ knockout mice (and $MAGL^{+/+}$ wild-types) were administered AOM (10mg/kg) and were exposed to 2 cycles of 2.5% DSS in their tap drinking water (105) one in the 1st, and the second in the 4th week of the experiment. Tumors were evaluated in the 13th week of the experiment.

Spontaneous tumor growth was examined by repeated AOM injections (6x) once weekly at the dosage of 10mg/kg in the first 6 weeks of the experiment. Mice were sacrificed after 30 weeks and total tumor size was determined as described above.

2.1.4. Open field test

The open field test was done as previously described (106). Briefly, mice were placed in the middle of an opaque gray plastic box (50 × 50 × 30 cm, length × width × height) and their behavior during a 5 minutes test session was recorded and tracked by a video camera and the VideoMot2 tracking software (TSE Systems, Bad Homburg, Germany). The ground area of the box was divided into a 36 x 36 cm central area and a surrounding outer area. Time spent in the central area was used to assess anxiety-like behavior and total distance travelled was measured to evaluate locomotor activity.

All mouse models were approved by the Austrian Federal Ministry of Science and Research (protocol numbers: BMWF-66.010/0039-II/3b/2013, BMWF-66.010/0008-II/3b/2014, BMWF-66.010/0037-II/3b/2013 and BMWF-66.010/0101-II/3b/2013) and performed in accordance with international guidelines. Great care was taken to minimize all suffering and pain.

2.2. Myeloperoxidase activity assay

Myeloperoxidase activity was determined as previously described (107) with minor modifications. Colon samples were placed into hexadecyltrimethylammonium bromide (HTAB) (Sigma-Aldrich, St.Louis, Missouri, USA) buffer (pH=6) containing 50mM KH_2PO_4 and 50mM K_2HPO_4 (both from Merck, Darmstadt, Germany) for thawing. The samples were mechanically homogenized in the buffer (still keeping the sample on ice) and afterwards centrifuged for 20 minutes at 9000 X g at 4°C. 10µL of supernatant were used for the assay and measured in triplicates in a 96-well plate. 200µL of a solution containing 10% phosphate buffer, 0.0167% o-dianizidine peroxidase substrate (Sigma-Aldrich, St.Louis, Missouri, USA) and 0.06% of H_2O_2 (Sigma-Aldrich, St.Louis, Missouri, USA) were added to the wells and the absorbance was measured on 450nm on a Microplate Spectrophotometer after 25 minutes (BioRad Hercules, California, USA).

2.3. RNA isolation and real-time reverse transcriptase PCR from mouse colon samples

The mRNA was extracted using Dynabeads® mRNA Direct^{tm} Kit (Life Technologies) according to manufacturer's protocol in order to eliminate DSS residues, after which the concentration was determined on a Nanodrop spectrophotometer (Nanodrop, Wilmington, Delaware, USA). 1µg of mRNA was used for cDNA transcription using the High Capacity cDNA Reverse Transcription Kit (Thermo Scientific, Waltham, Massachusetts, USA). The RT-PCR program was performed according to the manufacturer's instructions. Fast SYBR® Green PCR Master Mix (Applied Biosystems) was used for quantitative PCR, following manufacturer's instructions. The primers used are listed in Table 1 (108,109). The specificity of the PCR products was assessed by melting curve analyses which showed only single amplified products (108). Real-time PCR data was analyzed by the $2^{-\Delta\Delta ct}$ method (110).

Table 1 – primers used for PCR experiments

IL 1β	forward	5′- GGACATAATTGACTTCACCATGGAA 3′
	reverse	5′-CAGTCCAGCCCATACTTTAGGAA-3′
Cyclophilin	forward	5′-TTCCAGGATTCATGTGCCAG-3′
	reverse	5′-CCATCCAGCCATTCAGTCTT-3′
COX-2	forward	5'-CATGATCTACCCTCCCCACG-3'
	reverse	5'-CAGACCAAAGACTTCCTGCCC-3'
IL 6	forward	5′-TAGTCCTTCCTACCCCAATTTCC-3′
	reverse	5′-TTGGTCCTTAGCCACTCCTTC-3′

2.4. RNA isolation and real-time reverse transcriptase PCR from J774.1 mouse macrophages

Cells were frozen in liquid nitrogen and lysed in RNA buffer. Total RNA was then extracted using QIAshredder and RNeasy Kit (QIAGEN, Hilden, Germany), following the manufacturer´s instructions. RT-PCR was performed with 1 µg of total RNA and a High Capacity cDNA Reverse Transcription Kit (Applied Biosystems, Life Technologies, Grand Island, NY, USA) for cDNA transcription. Quantitative PCR (qPCR) was performed using SYBR® Green and GPR55 primers (#100-25636) from BioRad according to the manufacturer´s instructions. Amplicons were electrophoresed in 1% agarose gel and stained with ethidiumbromide.

2.5. Haematoxylin staining

Colon samples were taken and kept in Roti®-Histofix 10 % (Lactan, Graz, Austria) for 48 hours, after which they were rehydrated in running water for approximately 1 hour. The dehydration steps included 4 hours dehydration in 50% ethanol, 4 hours in 70% ethanol and overnight dehydration in 80% ethanol. On the second day, samples were kept for 3 hours in 96% ethanol, 2 hours in 100% ethanol, and then every half an hour changed from 50% ethanol/50% n-butyl acetate (Lactan, Graz, Austria), 100% n-butyl acetate solution, 50% n-butyl acetate/50% paraffin respectively. They were kept in paraffin (Roth, Karlsruhe, Germany) overnight in a pre-heated oven at 70°C. On the next day, the samples were embedded in paraffin and cut at 5 µm on the microtom (Microm, Walldorf, Germany) on the following day. Sections were mounted on superfrost ultra plus slides (Thermo Scientific, Waltham, Massacusetts, USA). After overnight drying, the slides were incubated in Gill No.2 haematoxylin solution (Roth, Karlsruhe, Germany) for 1 minute and afterwards placed in a chamber filled with tap water where they were incubated for another 10 minutes. The next day, the slides were incubated in xylol (Roth, Karlsruhe, Germany) and 5 minutes in each of the ethanol solutions (50%, 70%,

80%, and 100%) before submitting them to haematoxylin staining and immunohistochemistry.

2.6. Protein concentration determination of colon samples

Frozen samples were mechanically crushed with a bio-pulveriser from Biospec products (Bartlesville, Oklahoma, USA), and transferred into an Eppendorf tube containing 300µL of extraction buffer which consisted of 50mM Tris (Roth, Karlsruhe, Germany), 10mM EDTA (Roth, Karlsruhe, Germany), 1% TritonX-100 (Roth, Karlsruhe, Germany), and protease/ phosphatase inhibitors (Roche, Basel, Switzerland) according to manufacturer's instructions. Samples were then homogenized using an Ultra Thurax (IKA, Staufen, Germany) and afterwards centrifuged at 9000 X g for 10minutes on 4°C. The supernatants were collected and stored at -80°C. For protein concentration determination purposes, a part of the supernatant was diluted 1:100 and 100µL of the diluted sample was added in triplicates to a 96-well plate. A bovine serum albumin (Sigma-Aldrich, St.Louis, Missouri, USA) stock solution of 1mg/mL was prepared, and five different concentrations (0.8 – 6.4µg/100µL) were used to form the standard curve. Protein was determined with the BioRad Protein Assay Kit II, according to the instructions of the manufacturers, using a Microplate Spectrophotometer (BioRad Hercules, California, USA).

2.7. Cytokine determination in colon samples

To determine the contents of different cytokines (tumor necrosis factor α (TNF-α), interleukin 1β (IL-1β), interleukin6 (IL-6)), an enzyme linked immunoabsorbent assay (ELISA) (Ready-SET-Go!, eBioscience (San Diego, California, USA) was used, following the manufacturer's instructions.

2.8. Western blot analysis

30µg of protein extracts were diluted 1:1 with sample buffer containing 100mM TRIS/HCL and 5% SDS (Roth, Karlsruhe, Germany), 15% Glycerol, 0.004% Bromphenolblue and 5% Mercaptoethanol (all from Sigma-Aldrich, St.Louis, Missouri, USA). The samples were run on 12% polyacrylamide gels. The transfer was carried out using Invitrogen´s iBlot device (Waltham, Massachusetts, USA). Afterwards, the membrane was blocked for 1 hour in 5% blocking solution (1mM $CaCl_2$, 135mM NaCl, 2.5mM KCl, 25mM Tris-HCL, 0.1% [v/v] Tween20 and 5% milk powder) and incubated with the first antibody overnight at 4°C followed by 1 hour incubation in the secondary antibody at room temperature. The following antibodies were used: rabbit anti-Cox-2 (1:250, Abcam, Cambridgje, UK), rabbit anti-pSTAT3 and tSTAT3 (both 1:1000, Cell Signaling, Danvers, Massachusetts, USA) mouse anti-β-actin (1:7500, Sigma, St.Louis, Missouri, USA), goat anti-rabbit and goat anti-mouse secondary antibodies (1:5000 and 1:4000 respectively; Jackson Immuno Research, West Grove, Pennsylvania, USA). The proteins were visualized with Pierce ECL Western blotting substrate (Thermo Scientific, Waltham, Massachusetts, USA). Blots were analyzed for quantification with ImageJ Software (NIH, Bethesda, Maryland, USA).

2.9. Isolation of lamina propria leukocytes and flow cytometer analysis

The method was conducted as previously described (104,111). The colon was opened longitudinally, rinsed in HBSS (Life Technologies), and cut into small pieces (5mm) that were put in a 50 mL falcon containing HBSS (CMF), HEPES (Life Technologies) and Penicillin/Streptomycin (PS) (Sigma). The falcons were then put on a rotator at 37°C and the samples were washed 4x every 10 minutes with fresh HBSS/HEPES/PS, followed by 4x washes of 20 minutes with HBSS/EDTA/PS (EDTA from Life Technologies). Afterwards, the samples were washed in complete RPMI medium, (Life Technologies) for 5 minutes and then transferred into complete RPMI containing 100 units/mL of collagenase type 2

(Thermo Scientific, Waltham, Massacusetts, USA) for 1 hour (until tissue was almost transparent) at 37°C. The cell suspension was passed through a 40µm cell strainer into a new falcon tube and centrifuged at 400xg for 7 minutes. The pellet was washed with PBS (CMF) and leukocytes were stained with Alexa Fluor 647-conjugated CD11b Ab (1:100), PE-conjugated Siglec F Ab (1:100), Alexa Fluor 488-conjugated F4/80 Ab (1:20). All antibodies were purchased from eBioscience (San Diego, California, USA). The leukocytes were stained for 30minutes at 4°C, and afterwards washed with PBS (Life Technologies). After the washing step, fixative solution was added and cells were analyzed on a FACSCalibur flow cytometer (Becton Dickinson, California, USA). Data were normalized to colon weight and are expressed as percentage of total living cells.

2.10. Immunohistochemistry

Paraffin-embedded colon sections were prepared the same way as for the haematoxylin staining. After overnight drying of the paraffin-cut sections, they were deparaffinised in xylol (VWR, Radnor, Pennsylvania, USA) and dehydrated in descending alcohol concentrations (100%, 80%, 70%, 50%) each time 10 minutes. The sections were microwaved 2 x 5minutes in sodium citrate buffer (10mM sodium citrate (Merck, Darmstadt, Germany)), 0.05% tween 20 (Sigma), pH 6.0), and further processed by the ABC method according to manufacturer's instructions (Vector Labs, Burlingame, CA, USA). Sections were then incubated with anti-CD3 (1:1000, Serotec, Kidlington, UK), and anti-F4/80 (1:100, Serotec, Kidlington, UK), visualized with 3-3'-diaminobenzidine and counterstained with haematoxylin. Images were taken with an Olympus DP 50 camera, and processed with Cell^A imaging software (Olympus, Vienna, Austria). Only brightness and contrast of the entire picture were adjusted.

2.11. Stimulation of J774.1 mouse macrophages

The method was conducted as previously described (109) with slight changes. Cells were seeded in 6-well plates and at 80% confluence and starved overnight with serum free media. 30 minutes before stimulation with 0.1μM Phorbol 12-myristate 13-acetate (Sigma-Aldrich, St.Louis, Missouri, USA) for 2 hours, CID16020046 (or vehicle) was added to the cells at three different doses (1, 5 and 10 μM). Cells were afterwards snap-frozen in liquid nitrogen. Changes in Cox-2 expression (1:250, Abcam, Cambridge, UK) were evaluated via Western Blot.

2.12. CD11b expression in J774.1 mouse macrophages

Approximately 2 x 10^6 cells were put in 500μL of PBS and preincubated for 30 minutes with 1, 5, 10, 20 μM CID16020046. Cells were then stimulated with 1nM of MCP-1 (Peprotech, Rocky Hill, New Jersey, USA) for 30 minutes, and 1, 2, 4 hours in a 37°C water bath. Fifteen μl of Alexa Fluor 647 anti-mouse CD11b (BD Biosciences, Franklin Lakes, New Jersey, USA) was added 15 minutes before the end of the incubation time. After adding the fixative solution, the cells were measured on the FACSCalibur flow cytometer. Data were expressed as percentage change to the vehicle treatment.

2.13. Migration of J774.1 mouse macrophages

Migration assays with J774.1 cells were performed in 24-well Transwell plates with 8 μm membrane inserts (Corning Inc., Lowell, MA, USA). Cells were starved in DMEM containing 0.5% FBS (Life Technologies) overnight and then incubated with CID16020046. A suspension of 3 x 10^5 cells was placed in the upper compartment, and C5a (5 nM; Sigma) (1) was added to medium as a chemoattractant to the lower compartment. Cells were allowed to migrate for 2 hours at 37°C and 5% CO_2 in a humidified incubator. Upon completion of migration, the upper sides of the filters were cleaned with a cotton swab, and filters

were dried and fixed in formaldehyde for 30 minutes. After a wash in PBS, filters were mounted and coverslipped in Vectashield ® (Vector Labs). Cell nuclei were counted under a fluorescent microscope (Olympus IX 70). Each migration experiment was performed in duplicates. The average number of migrated cells was determined from at least three independent experiments.

2.14. Neutrophil chemotaxis

Isolated human neutrophils were resuspended in phosphate buffered saline (Ca^{++} and Mg^{++} free) at a density of 2 x 10^6 cells/mL. The chemoattractant (27µL) (100nM Formyl-Methionyl-Leucyl-Phenylalanine (fMLP)) or PBS(-) was placed in the bottom well of a 48-well microBoyden chamber. A 5µm polycarbonate membrane was preincubated in PBS(-). The cell suspension (45µL) was placed into the upper wells of the chemotaxis chamber. The chamber was afterwards incubated at 37°C for 1hour. The remaining cells were removed from the upper compartment of the chamber, the chamber was reassembled and the cells of the lower compartment were placed into polypopylene micro tubes. Fixative solution (150µL) was added and the samples were analyzed by the flow Cytometer.

2.15. Data analysis

All statistical analysis was performed using Prism 4.03 (GraphPad Software, USA). Experimental data were analyzed either by one-way ANOVA with Bonfferoni multiple comparison post-test or Student's t-test. Significance was defined as $P<0.05$.

3. Results

3.1. Antagonism and genetic deletion of GPR55 and decreases the inflammatory macroscopic score and MPO activity in DSS and TNBS colitis

In preliminary experiments, different dosages of CID16020046 were tested, to determine an effective dose of the GPR55 inhibitor for the *in vivo* DSS colitis model (Figure 7A). Only a dosage of 20 mg/kg (s.c.) of CID16020046 induced a significant reduction of the inflammatory macroscopic score of around 40%, and this dosage was, therefore, used for all further *in vivo* experiments. Inhibition of GPR55 pharmacologically (Figure 7B) or genetically (Figure 8A) decreased the macroscopic score significantly in the DSS model. The GPR55 inhibitor was also used in a different colitis model, a model of TNBS colitis, and led to the same effect as in the DSS colitis model, namely to a significant decrease in the macroscopic score compared to the vehicle (DMSO)-treated group (Figure 7C). To investigate whether the macroscopically observed effect of CID16020046 changed inflammatory markers, MPO activity was assessed and revealed a significantly decreased activity in CID16020046-treated animals in both the DSS and TNBS colitis models (Figure 7D and E). Haematoxylin staining of colon sections from DSS (Figure 7F) and TNBS (Figure 8B) -exposed animals showed a more preserved architecture of the crypts and a thinner submucosal layer after CID16020046 treatment, confirming the macroscopic observation of an improvement of colitis in CID16020046-treated animals. In the TNBS model of colitis, reduction in the macroscopic score in GPR55$^{-/-}$ mice compared to their wild-type littermates, did not reach significance (Figure 8C).

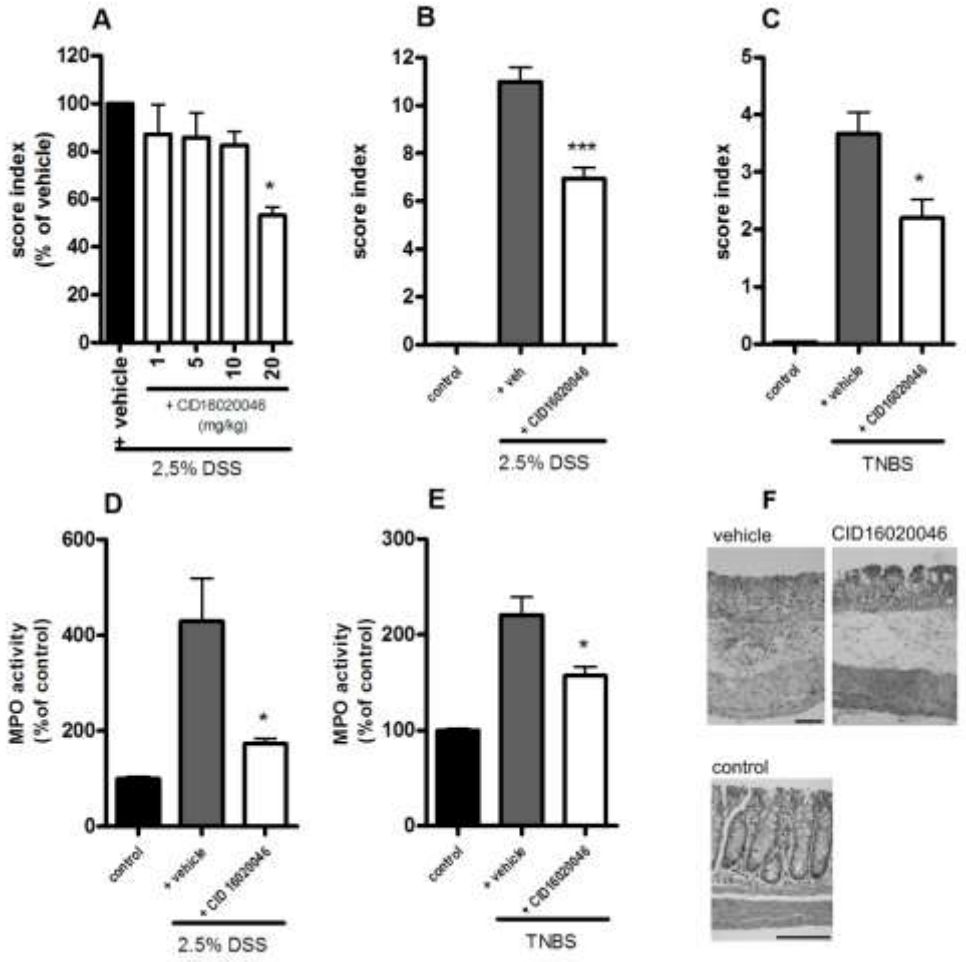

Figure 7

Pharmacological inhibition of GPR55 in the DSS colitis model decreases the inflammatory macroscopic score and the MPO activity, as well as the macroscopic score and MPO activity in the TNBS colitis model

Macroscopic evaluation of DSS colitis was performed at different dosages of the GPR55 inhibitor CID16020046 to determine an effective dosage **(A)** (n=4-10, one-way ANOVA; *p<0.05). The dosage of 20 mg/kg (s.c.) was used for all further *in vivo* experiments. Macroscopic scores for the DSS **(B)** (n=5-17, one-way ANOVA; ***p<0.001) and TNBS **(C)** (n=6-16, one-way ANOVA; *p<0.05) colitis models revealed a decreased macroscopic score for CID16020046 treated animals. Myeloperoxidase (MPO) activity was determined to evaluate the severity of inflammation in both colitis models **(D, E)** and was decreased in CID16020046-treated animals (n=3-10 and 3-16, one-way ANOVA; *p<0.05). Haematoxylin staining of colon sections from animals treated with GPR55

inhibitor revealed a more preserved architecture of crypts together with reduced muscle thickness compared to the vehicle animals **(F)**.

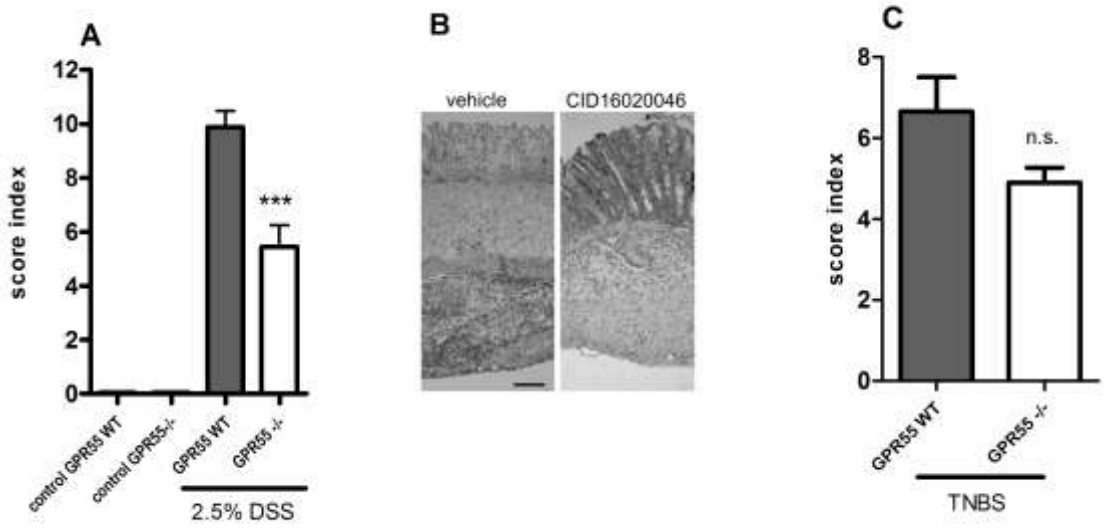

Figure 8

Genetic deletion of GPR55 is protective in the DSS colitis model

GPR55$^{-/-}$ knockout mice had a significantly decreased macroscopic score compared to their GPR55 $^{+/+}$ wild-type littermates **(A)** in the DSS model of experimental colitis (n=3-9, one-way ANOVA; ***p<0.001). Haematoxylin staining of colon sections from animals TNBS colitis revealed a more preserved architecture of crypts together with reduced muscle thickness after treatment with GPR55 inhibitor compared to the vehicle group **(B)**. GPR55$^{-/-}$ knockout mice showed no significant difference in the macroscopic score index compared to the wild-type animals in the TNBS colitis (n=11-15, Student´s t-test; not significant (n.s.)) probably because of the low sample size **(C)**. WT indicates GPR55 $^{+/+}$.

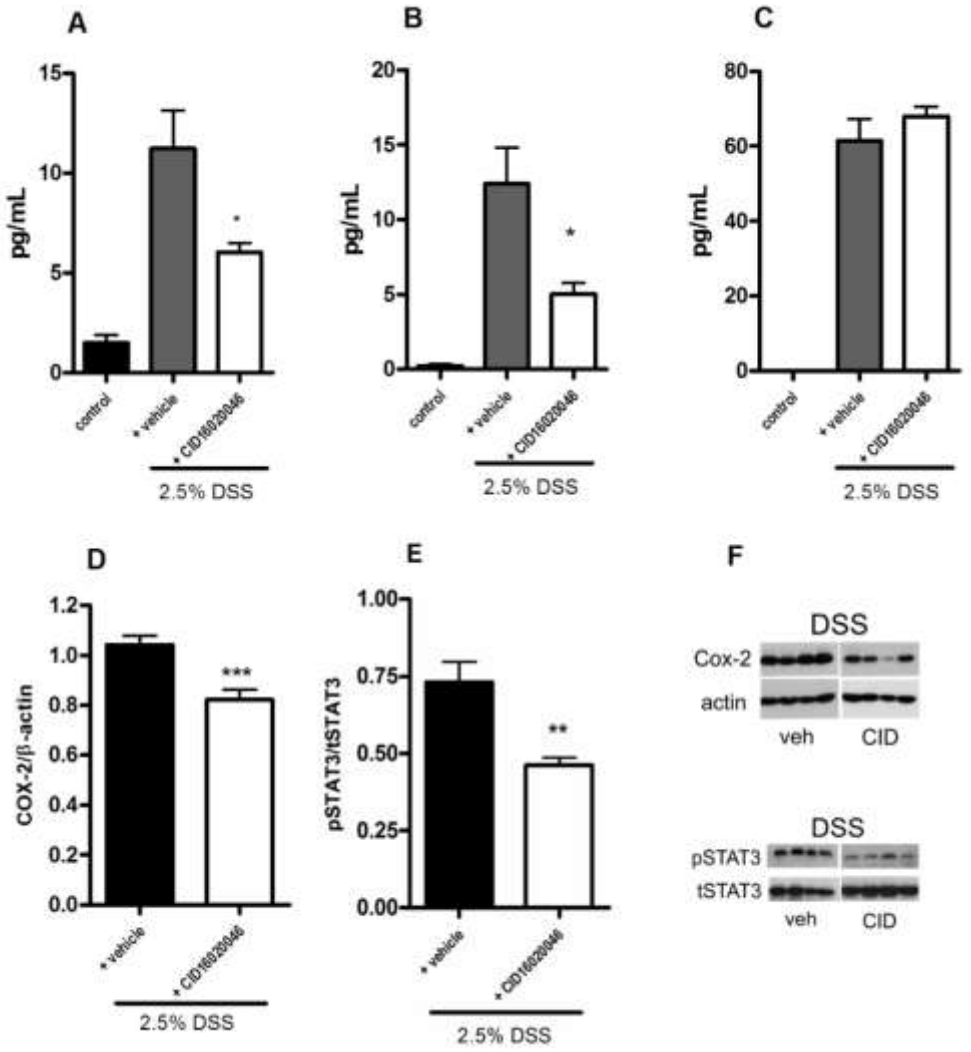

Figure 9

Treatment with GPR55 inhibitor CID16020046 reduces proinflammatory cytokines and markers in DSS colitis TNF-α **(A)**, IL-1β **(B)** and IL-6 **(C)** levels were examined in the colon tissue of DSS-treated mice after treatment with the GPR55 inhibitor CID16020046 (n=3-10, one-way ANOVA, *p<0.05). Western blots of whole colon tissue demonstrated reduced Cox-2 expression after treatment with CID16020046 in the DSS colitis **(D)**. Representative blots of DSS colitis show bands of Cox-2 in colon tissue from four animals **(F)**. Band densities of samples were normalized to

actin (n=6-12, Student´s t-test; ***p<0.001). pSTAT3 levels were reduced in the DSS colitis model for the inhibitor treated group **(E)**. Representative blots show bands of pSTAT3 in colon tissue from four animals **(F)**. Band densities of samples were normalized to total STAT3 (tSTAT3) (n=6, Student´s t-test; **p<0.01

3.2. Treatment with GPR55 antagonist CID16020046 alters proinflammatory cytokine profile and expression of proinflammatory markers in DSS and TNBS colitis

I next explored the effects of CID16020046 in more detail and used the colonic tissue of DSS and TNBS colitic mice to measure possible changes in the proinflammatory cytokine levels. In the DSS colitis model, inhibition of GPR55 caused significant reductions in TNF-α and IL-1β levels (Figure 9 A and B) whilst IL-6 levels stayed unaltered. Mice that underwent TNBS colitis revealed a distinct cytokine profile. IL-1β and IL-6 levels were significantly decreased in CID16020046 treated animals (Figure 10 B and C) while TNF-α levels also decreased, however, not significantly (Figure 10A). To investigate changes in Cox-2 levels, Western blots of whole colon protein extracts were performed. In both colitis models, Cox-2 expression was significantly decreased in CID16020046-treated animals (Figure 9D and F and Figure 10 D and F) but interestingly, GPR55 inhibition produced different effects on STAT3 phosphorylation showing a decrease in the DSS, but an increase in the TNBS colitis model (Figure 9E and Figure 10E).

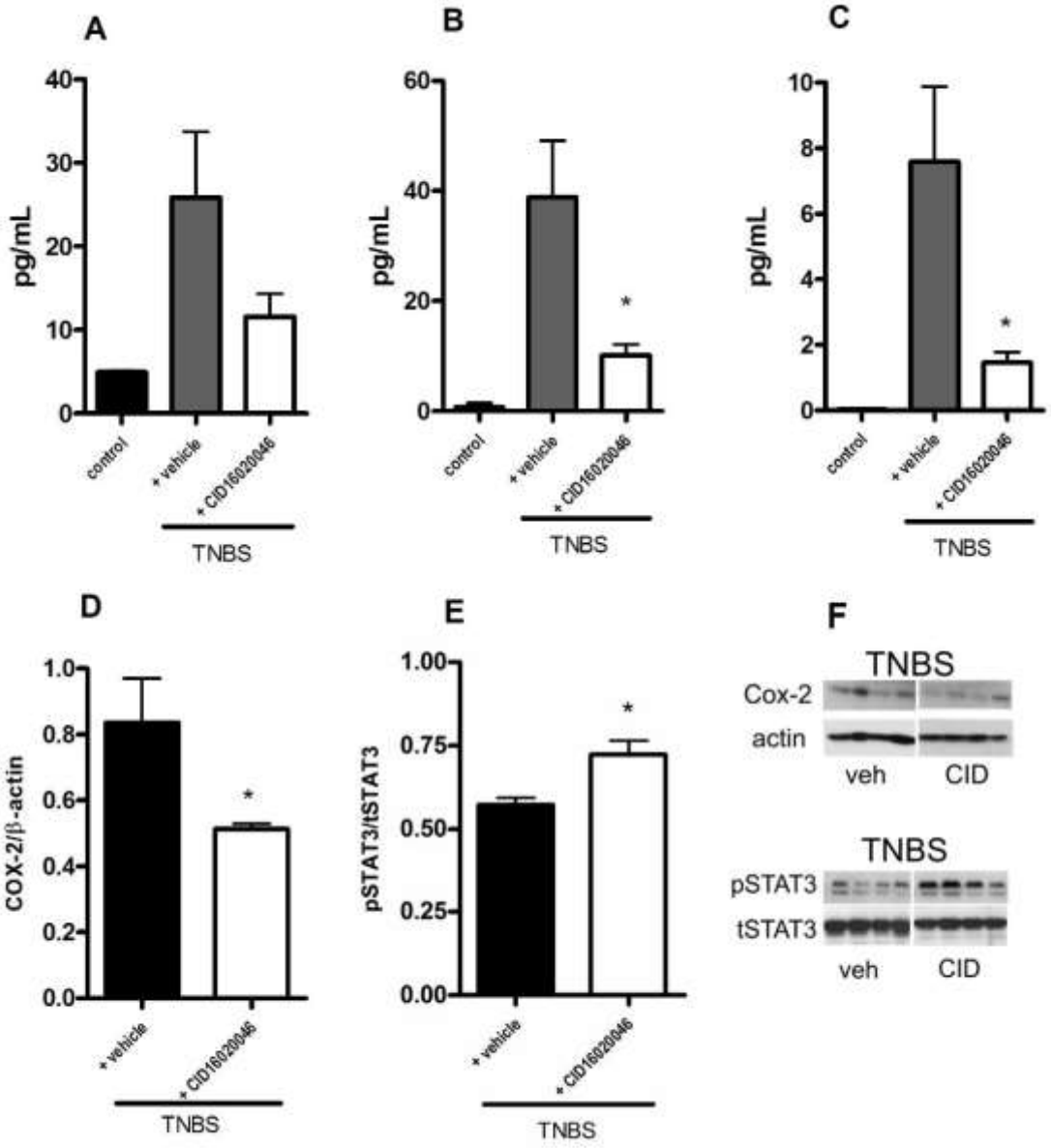

Figure 10

CID16020046 treatment induces an increase in pSTAT-3 but a decrease in proinflammatory cytokines in the TNBS model

In the TNBS model, IL-1β **(B)** and IL-6 **(C)** levels were significantly decreased while TNF-α levels **(A)** were also lowered, however not significantly, after treatment with CID16020046 (n=4-15, one-way ANOVA; Tukey´s multiple comparison *p<0.05). Western bots of whole colon tissue demonstrated reduced Cox-2 expression after treatment with CID16020046 in the TNBS colitis **(D)**.

Representative blots show bands of Cox-2 in colon tissue from four animals **(F)**. Band densities of samples were normalized to actin (n=6-12, Student´s t-test; ***p<0.001). pSTAT3 levels were increased in the TNBS colitis model **(E)** for the GPR55 inhibitor-treated group. Representative blots show bands of pSTAT3 in colon tissue from four animals **(F)**. Band densities of samples were normalized to total STAT3 (tSTAT3) (n=6, Student´s t-test; *p<0.05).

3.3. GPR55 inhibitor CID16020046 alters leukocyte recruitment into the lamina propria of DSS-colitic mice

I next measured and quantified leukocyte recruitment into the lamina propria in the DSS colitis model (Figure 11). GPR55 inhibition by CID16020046 significantly decreased the infiltration of lymphocytes (Figure 11A) and macrophages (Figure 11B), whilst interestingly increasing the number of infiltrating neutrophils as compared to the vehicle treatment (Figure 11D). No changes in the number of infiltrating monocytes (Figure 11C) and eosinophils (Figure 11E) were observed.

To visually demonstrate the leukocyte populations that were found reduced in the recruitment experiment, immunohistochemical staining for the T lymphocyte marker CD3 and the macrophage marker F4/80 was employed and revealed significantly decreased immunoreactivity in the colon submucosa after GPR55 inhibitor treatment (as compared to treatment with vehicle) (Figure 11F).

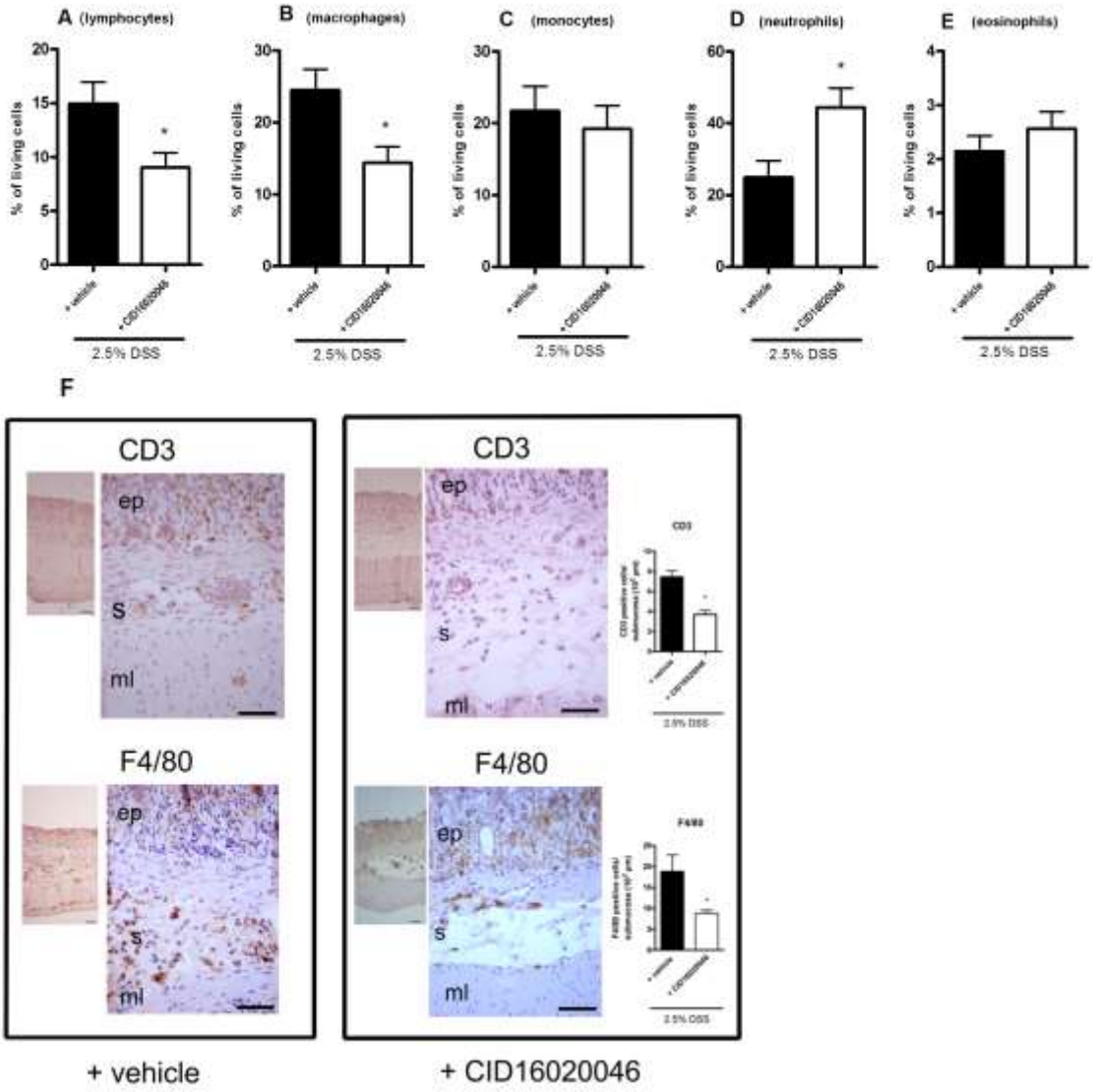

Figure 11

Leukocyte recruitment into the colon in DSS colitis is modulated by CID16020046

CID16020046 inhibited lymphocyte **(A)** and macrophage **(B)** infiltration into the lamina propria of the colon in DSS-colitic mice while the number of monocytes **(C)** and eosinophils **(E)** stayed unaltered. Neutrophils showed increased influx upon CID16020046 treatment **(D)** (n=9, Student´s t-test; *p<0.05). F4/80 and CD3 staining is also reduced in the submucosa of GPR55 inhibitor-treated mice as compared to the vehicle-treated ones **(F)**. Images are representative of sections from 3 different mice from each group; ep, epithelium; mm, muscularis mucosae; sm, submucosa. For cell counting, 6-10 sections from non-overlapping areas (from 3 different mice each group) were used (*p<0.05; Student's t-test).

3.4. GPR55 inhibitor CID16020046 alters leukocyte recruitment into the lamina propria of TNBS-colitic mice

After I have observed interesting effects of CID16020046 treatment on the infiltration of leukocytes into the lamina propria in the DSS-colitis model, I was also curious to see the effect of GPR55 inhibition on the infiltration of leukocytes in the TNBS-colitis model. However, GPR55 inhibition by CID16020046 was able to inhibit only lymphocytes infiltration (Figure 12A), while other cell populations were not affected by CID16020046 treatment (Figure 12 B-E).

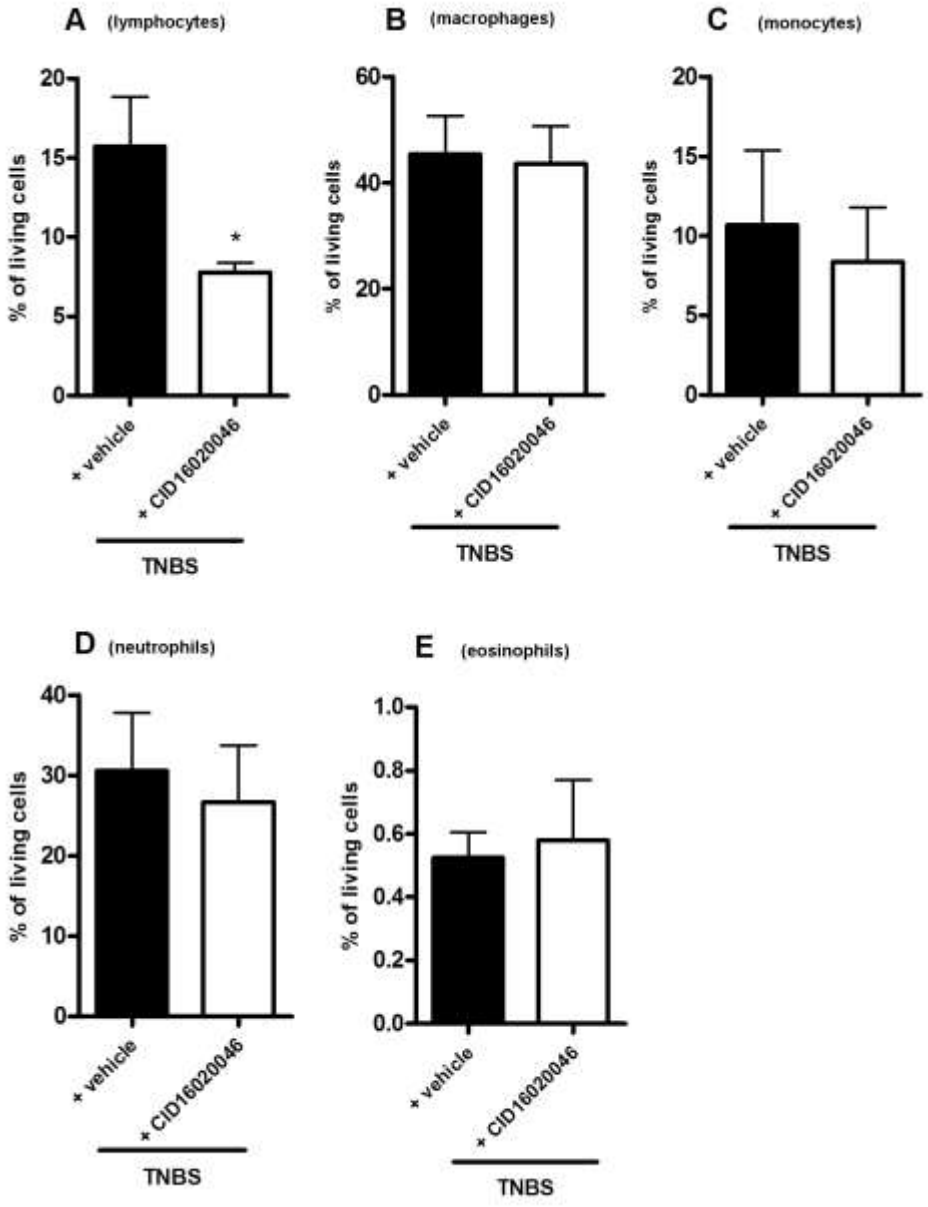

Figure 12

Only lymphocyte recruitment into the colon in TNBS colitis is modulated by CID16020046

CID16020046 inhibited lymphocyte **(A)** infiltration into the lamina propria of the colon in TNBS-colitic mice while the number of other cell populations (macrophages **(B)**, monocytes **(C)**, neutrophils **(D)** and eosinophils **(E)** stayed unaltered. n=5 (*p<0.05; Student's t-test).

3.5. GPR55 inhibitor CID16020046 modulates migration and activation of mouse macrophage cell line J774.1 and inhibits human neutrophil chemotaxis

Effects of CID16020046 observed *in vivo* were further investigated at a cellular level. Due to the prominent effect of CID16020046 on the macrophage recruitment in the DSS model, I determined effects of CID16020046 on the migration and inflammatory activity of the mouse macrophage cell line J774.1. This cell line showed high expression of GPR55 mRNA, as compared to RAW264.7 mouse macrophages, and was therefore used in the *in vitro* assays (Figure 13A). A concentration of 5nM of C5a induced the migration of J774.1 cells and this effect was concentration-dependently reduced after incubation with 1 and 5 μM CID16020046 (Figure 13B and C). Similarly, expression of CD11b, a β2-integrin that is rapidly activated and upregulated on the leukocyte membrane upon activation, was concentration-dependently decreased after incubation with 1-10 μM CID16020046 (Figure 13D). Treatment with 1 and 2.5 μM CID16020046 also strongly diminished migration of human neutrophils when using 100 nM of fMLP as a chemoattractant (Figure 13E).

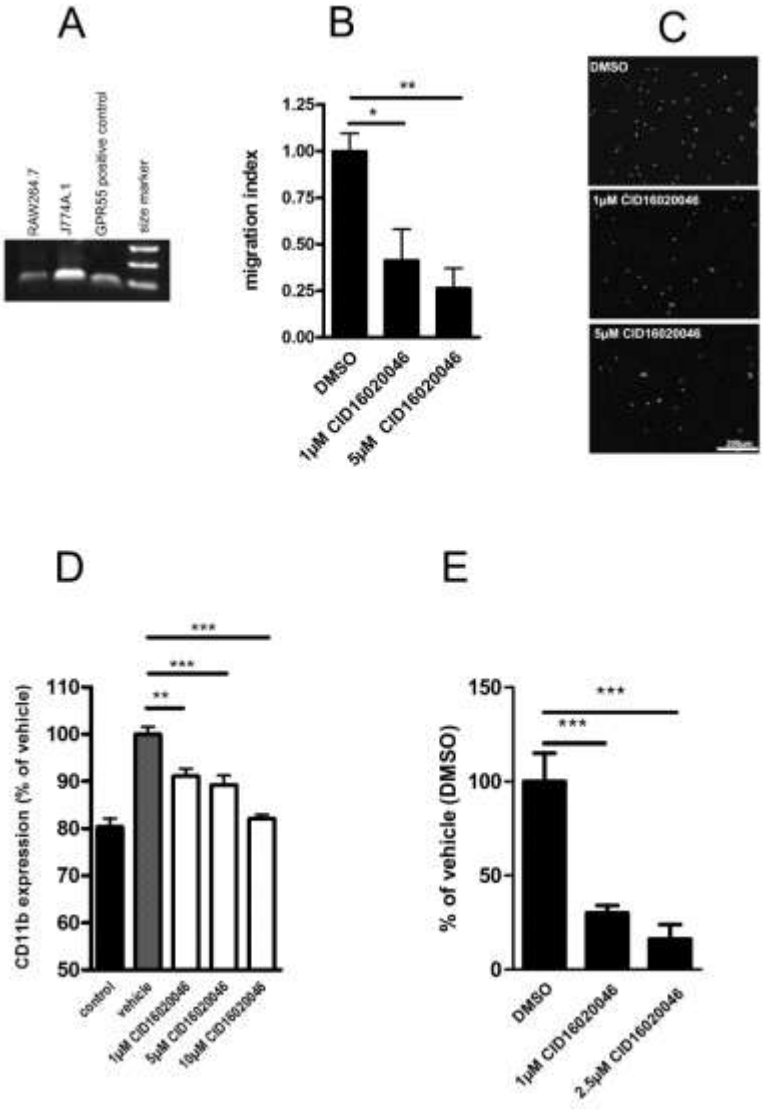

Figure 13

Effects of the GPR55 inhibitor CID16020046 on migration and activation of the mouse macrophage cell line J774.1

The PCR gels shows amplification of GPR55 transcripts in the mouse macrophage cell lines RAW264.7 and J774.1 using validated primers from BioRad GPR55 cDNA obtained from the manufacturer served as a positive control (#100-29101; BioRad). **(A)**. Amplicons were electrophoresed in 1% agarose gel and stained with ethidiumbromide. Transwell migration assays with J774.1 cells and 5nM of C5a as a chemoattractant showed a reduction in migration after incubation with 1 and 5 μM of GPR55 inhibitor CID16020046 (n = 4; ANOVA; Tukey's post-hoc

test) **(B)**. Representative images from cells that have migrated to the lower side of the migration filter are shown in **(C)**. For visualization and counting, cell nuclei were stained with DAPI; Size bar: 200 µm **(C)**. CD11b expression was concentration-dependently reduced by CID16020046 in J774.1 cells **(D)**. CID16020046 also reduced concentration-dependently human neutrophil migration **(E)**. Data are from three independent experiments; ANOVA; Tukey's post hoc test; *p<0.05, **p<0.01, ***p<0.001.

3.6. CID16020046 does not change the locomotor and anxiety behavior of healthy mice

Since GPR55 is widely expressed in the brain, it may be linked to motor behavior (112).

As GPR55 agonists have been also shown to exert central effects (113), we used an open field test to investigate whether CID16020046 would change the locomotor and anxiety behavior of mice. Daily treatment of healthy mice with 20 mg/kg of CID16020046 (6 x s.c.) did not alter their locomotor activity (Figure 14A) (measured as total travelling distance) or anxiety behavior (Figure 14B) (measured as time spent in the center of the box), as compared to vehicle-treated animals. Additionally, mean body weights and body temperatures did not differ between the treatment groups (Figure 14D and E) suggesting that CID16020046 does not induce central activity or sickness behavior.

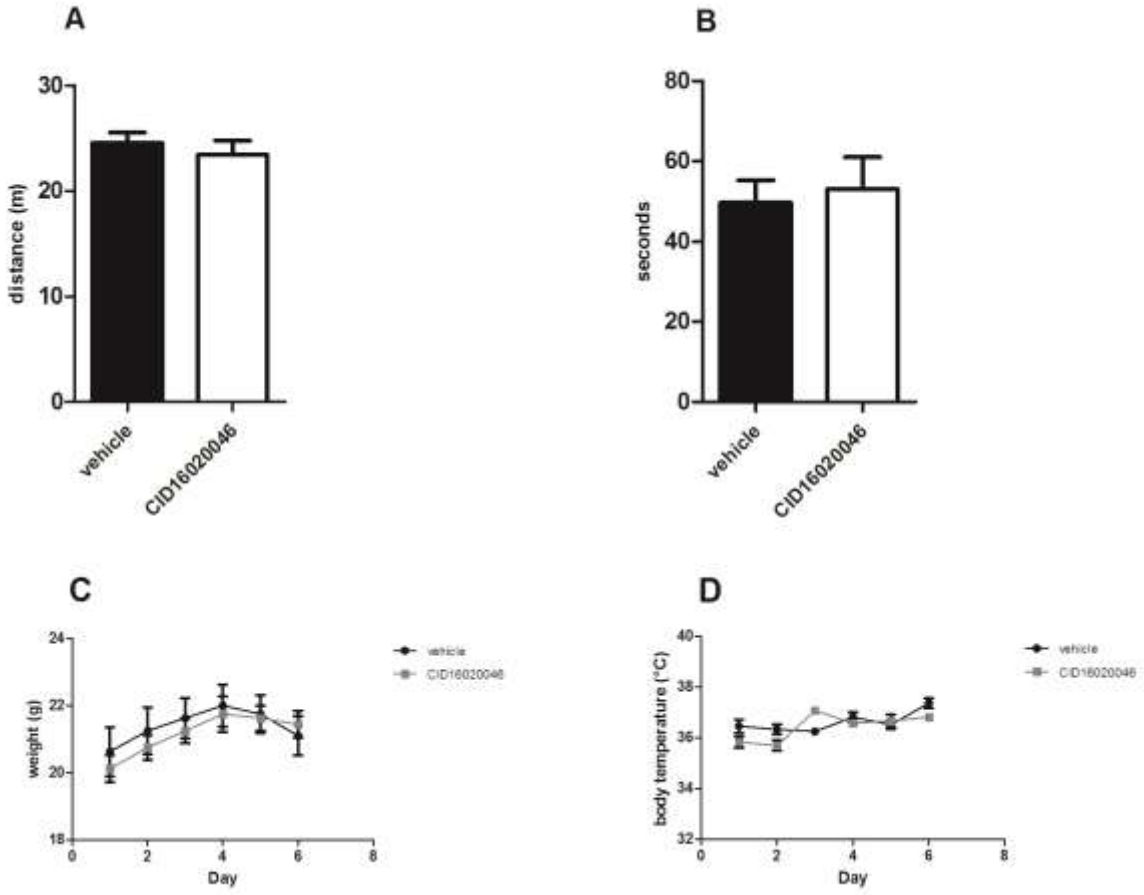

Figure 14

GPR55 inhibitor CID16020046 does not change locomotor and sickness behavior in healthy mice. Locomotor behavior of CID16020046 (20 mg/kg) - and vehicle (DMSO)-treated healthy mice was determined in an open field test as distance travelled within the plastic box (in meters; *m*) **(A)**. Anxiety behavior was measured as time spent in the center of the box (in seconds; *sec*) **(B)**. Body weight of healthy mice receiving CID 16020046- or vehicle (DMSO) was also measured daily and showed no change of weight **(C)**. In addition, a rectal thermometer was used to daily monitor the body temperature of mice receiving GPR55 inhibitor or vehicle. No differences in body temperature were observed between these two groups **(D)**.

3.7. Pharmacological and genetic inhibition of MAGL reduces severity of DSS colitis

According to the macroscopical evaluation of the disease severity, $MAGL^{-/-}$ knockout mice showed less severe colitis after being exposed to 2.5% DSS as compared to their $MAGL^{+/+}$ wild-type littermates (Figure 15A). The macroscopical observation was confirmed microscopically by hematoxylin staining of colon sections from DSS-exposed animals, which revealed a more preserved architecture of crypts together with reduced muscle thickness in $MAGL^{-/-}$ knockout compared to $MAGL^{+/+}$ wild-type mice (Figure 15G).

I was curious to see whether the same effect could be achieved by pharmacological inhibition of the MAGL enzyme. Thus, 16mg/kg of the MAGL inhibitor JZL 184 (91) was applied once daily s.c. to the mice to examine the effects of the MAGL inhibitor on colitis. The results revealed a robust effect of the MAGL inhibitor on the macroscopic scoring of animals in which DSS colitis was induced (Figure 15B). When applied twice daily at the dosage of 16mg/kg (s.c.), JZL 184 caused a slightly bigger decrease compared to the once daily treatment of in the inflammatory macroscopic score as compared to the vehicle-treated animals (Figure 15C). Upon checking for a decrease in the Cox-2 levels in the colon, the effect of JZL184 that was observed macroscopically was supported by a reduced expression of Cox-2 mRNA in the inhibitor-treated animals as compared to the vehicle-treated mice (Figure 15D). Proinflammatory cytokine levels in JZL 184-treated animals were unaltered, but showed a high tendency towards a decreased expression with nearly significant p-values ($p=0.06$ for IL-1β and $p=0.09$ for IL-6, Figure 15E and F).

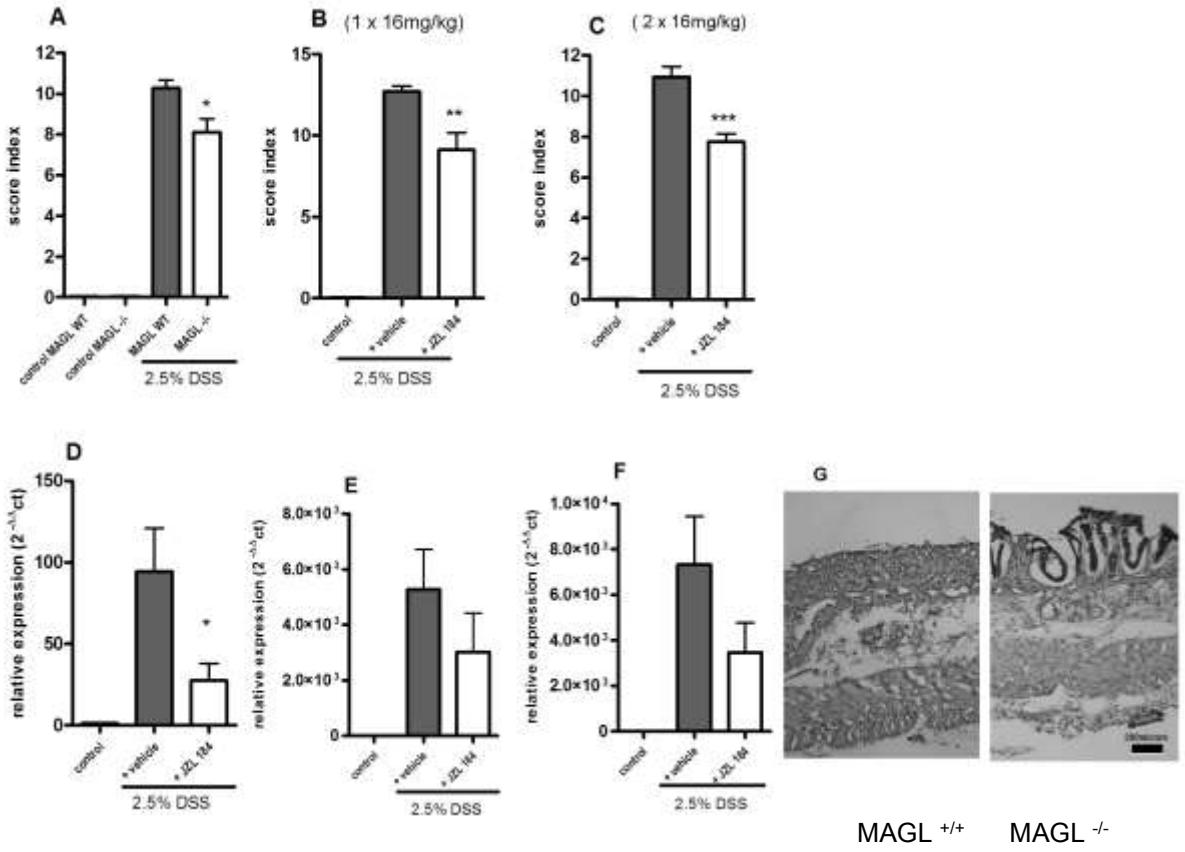

Figure 15

MAGL inhibition improves macroscopic inflammatory scores and reduces proinflammatory marker expression in DSS-induced colitis

MAGL$^{-/-}$ knockout mice showed a decreased macroscopic colitis score in comparison to their MAGL $^{+/+}$ wild-type littermates **(A)** (n=5-16, one-way ANOVA; Tukey's multiple comparison *p<0.05). Pharmacological inhibition of MAGL by JZL 184 in C57BL/6N at the dosage of 16mg/kg, given to the mice once **(B)** (n=5-8, one-way ANOVA; Tukey's multiple comparison **p<0.01) or twice daily s.c. **(C)** (n=5-16, one-way ANOVA; Tukey's multiple comparison ***p<0.001) also decreased the macroscopic scoring significantly. Mice treated with JZL 184 s.c. 2 x daily 16mg/kg also showed a decreased Cox-2 expression **(D)** determined by qPCR (n=3-7, one way ANOVA; Tukey's multiple comparison *p<0.05).). IL-6 **(E)** and IL-1β **(F)** expression levels in animals treated with the MAGL inhibitor were reduced, however, not significantly (n=3-7, one-way ANOVA; Tukey's multiple comparison p=0.09 and p=0.06). Hematoxylin staining of colon sections animals revealed a more preserved architecture of crypts together with reduced muscle thickness in DSS-exposed MAGL $^{-/-}$ knockout as compared to MAGL $^{+/+}$ wild-type mice **(G)**. WT indicates MAGL $^{+/+}$.

3.8. Pharmacological and genetic inhibition of MAGL inhibits tumor growth in a colitis-associated colon cancer model

Since there was an obvious effect on the colonic inflammation by inhibition of MAGL during DSS colitis, I was curious to see whether the inhibition of MAGL could inhibit tumor growth *in vivo* in a colitis-associated colon cancer model (105). Like in the DSS colitis model, mice received 16mg/kg of JZL 184 for 15 days i.p. and total tumor area per mouse was evaluated 9 weeks after DSS exposure (Figure 16A). No difference between the vehicle and JZL 184 treated group was observed (Figure 18A). A higher dose of the inhibitor was then used, since in the DSS colitis model, a twice daily application of 16mg/kg of JZL 184 s.c. had a stronger effect on the macroscopic scoring than the once daily treatment. Since in the colitis-associated colon cancer model, the mice received the inhibitor after the DSS exposure, I did not administer the drug twice daily, but in a single daily dose (Figure 16B). Administration of 32mg/kg of JZL184 s.c. did not show any significant difference to the vehicle-treated group regarding the total tumor area of the colon (Figure 18B). The administration of JZL 184, which started 3 days after the end of the DSS exposure acts at the very early stage of tumor initiation, and may have been too early to show any effect on the total tumor size at the end of the experiment. I, therefore, tried a different approach, and applied JZL 184 at two different later timepoints, the first between the week 6-8 (Figure 16C) of the experiment and the second in the weeks 8-10 (Figure 16D) of the experiment. An outline of the experiments is shown in Figure 16. Mice were sacrificed in the 9^{th} and 11^{th} week of the experiment, respectively. Treatment with JZL 184 reduced total tumor area of the colon only in the experiment in which JZL 184 was administered at the later timepoint, between weeks 8 and 10, indicating an effect of MAGL inhibition on tumor promotion rather than on tumor initiation (Figure 18 C and D). Genetic deletion of MAGL expression caused significantly less tumor growth as observed to MAGL $^{+/+}$ wild-type littermates (Figure 18E). The outline of the experiments is shown in Figure 17. MAGL $^{-/-}$ knockout mice were also exposed

to repeated AOM injections for 6 weeks to evaluate spontaneous tumor development without the inflammatory boost with DSS (outline of the spontaneous cancer experiment is shown in Figure 17B). MAGL $^{-/-}$ knockout mice revealed reduced total tumor area, but the difference to the MAGL $^{+/+}$ wild-type littermates did not reach significance (Figure 18F). The histopathological evaluation of the tumors by Prof. Dr. Johannes Haybäck (Institute of Pathology, Medical University of Graz) revealed no significant difference between MAGL $^{-/-}$ knockout and MAGL$^{+/+}$ wild-type tumors, which resemble human tubular adenomas. A representative histological picture of a hematoxylin stained section of a colon tumor (from a MAGL $^{-/-}$ knockout mouse) is shown in Figure 18G.

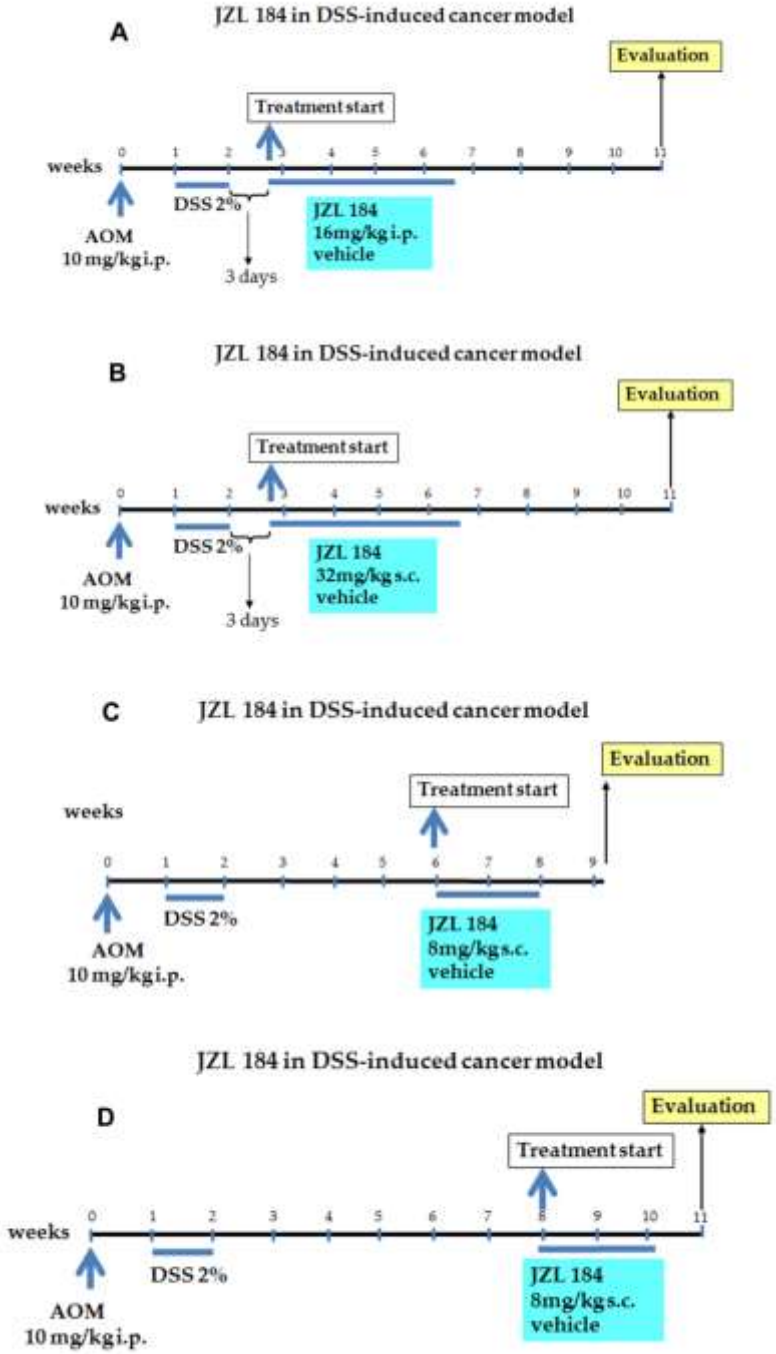

Figure 16

Outline of the colitis-induced cancer model with 16mg/kg i.p. of JZL 184 **(A)**, 32mg/kg s.c. of JZL 184 **(B)**, 8mg/kg s.c. JZL 184 between the weeks 6 and 8 **(C)** and 8mg/kg s.c. JZL 184 treatment between the weeks 8 and 10 **(D)**.

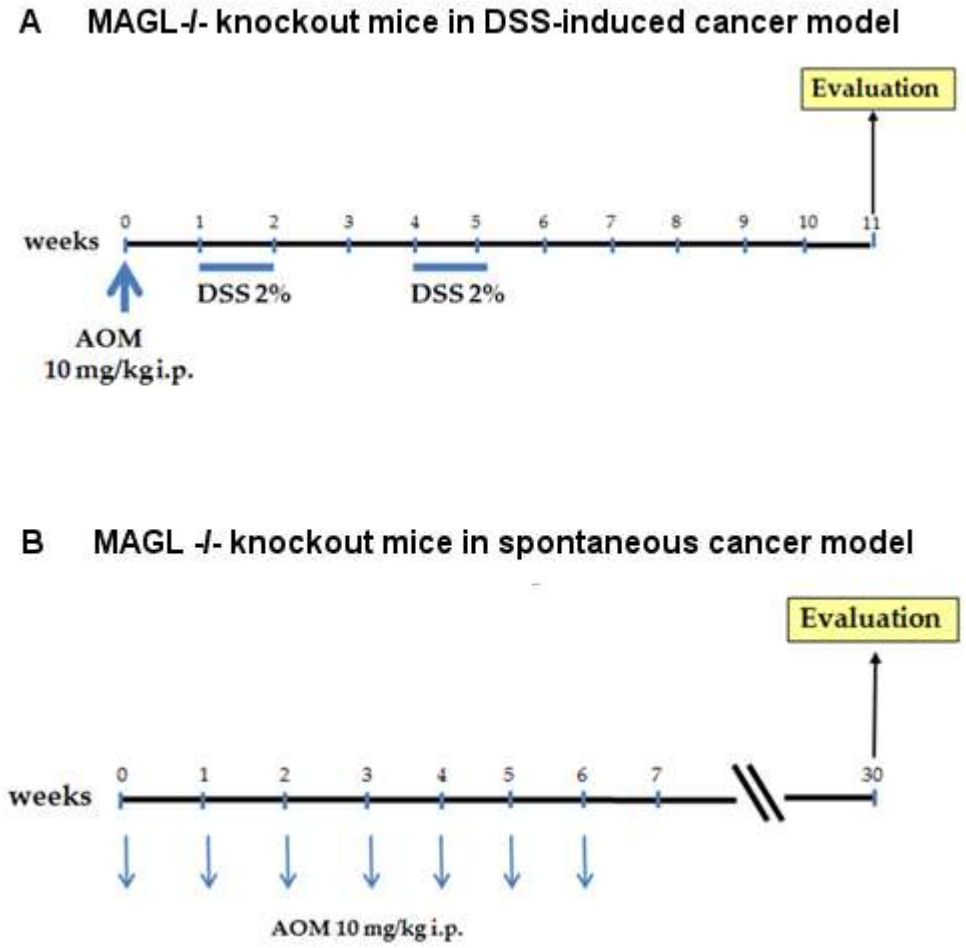

Figure 17

Outline of the colitis-induced cancer **(A)** and the spontaneous cancer model **(B)** in MAGL $^{-/-}$ mice.

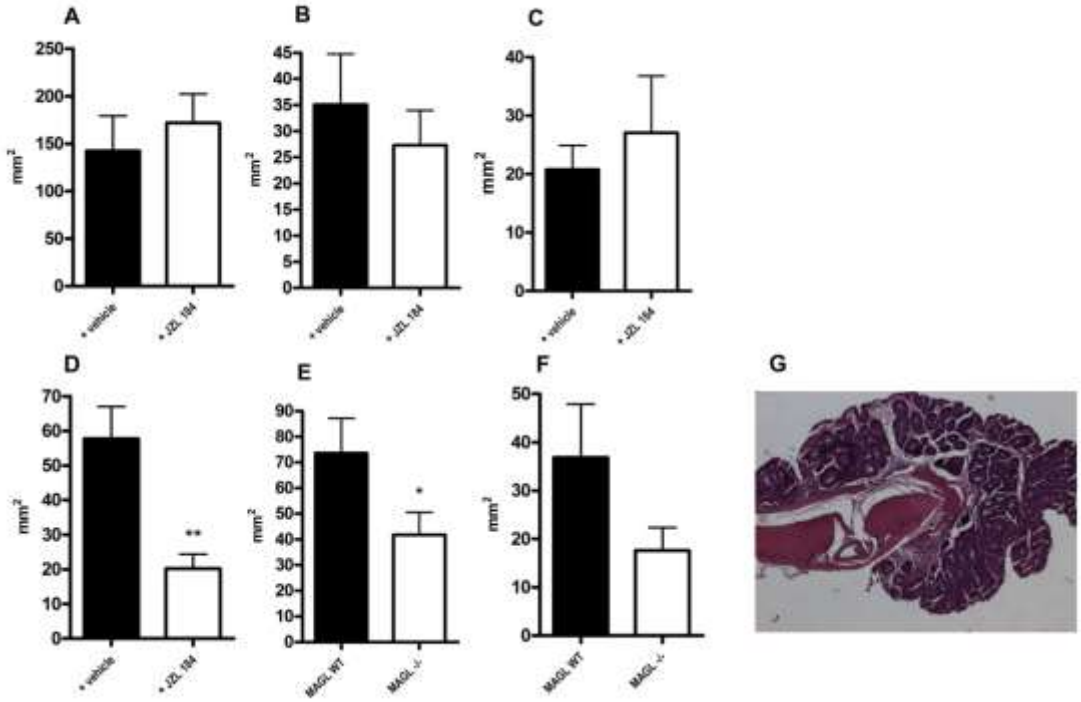

Figure 18

Genetic deletion and pharmacological inhibition of MAGL (at a low dosage) inhibits tumor growth in a colitis-induced cancer model

Treatment of CD1 mice with 16mg/kg (i.p.) **(A)** and 32mg/kg (s.c.) **(B)** JZL 184 in the colitis-induced cancer model showed no reduction of the total tumor area in comparison to the vehicle-treated group (n=8-9 and n=10, Student's t-test; p=n.s.) Treatment with a lower dose (8mg/kg (s.c.)) between the 4-6 weeks of the experiment did not reveal any difference between the vehicle and JZL 184 treated group either **(C)** (n=4-8, Student's t-test; p=n.s.). When JZL 184 was applied at a dosage of 8mg/kg (s.c.) and at a later time point (between weeks 6–8) **(D)**, mice showed a smaller total tumor area as compared to the vehicle-treated animals (n=4-8, Student's t-test; **p<0.01). MAGL $^{-/-}$ knockout mice showed a decreased total tumor area in the colitis-induced cancer model compared to their MAGL $^{+/+}$ wild-type littermates **(E)** (n=41-44, Student's t-test; *p<0.05). The spontaneous cancer model also demonstrated a tendency towards a reduced total tumor area, but failed to reach significance **(F)** (n=8-9, Student's t-test; p=0.13). A representative picture of a section from a colonic tumor stained with haematoxylin is shown on picture **G** (magnification x100) (courtesy of Prof. Dr. Johannes Haybäck). WT indicates MAGL $^{+/+}$.

4. Discussion

In this thesis, the role of two components of the EC system were investigated. First, the role of the GPR55 receptor in experimental colitis and then the role of the endocannabinoid 2-AG in experimental colitis and colitis associated cancer. The data revealed that GPR55, unlike the cannabinoids receptors CB1 and CB2, might play a proinflammatory role in experimental colitis in mice. Treatment with a selective GPR55 antagonist decreased the expression of inflammatory markers (TNFα, IL-1β, COX-2) in DSS and TNBS models of colitis as well as the influx of lymphocytes into the lamina propria. Through selective inhibition of MAGL, the main enzyme responsible for degrading 2-AG, mice had macroscopically less inflammation in DSS colitis, as well as reduced tumor growth in an colitis-associated cancer model.

4.1. Part 1 - Pharmacological and genetic inhibition of GPR55 in experimental colitis: Role of GPR55 in intestinal inflammation

GPR55 has been suggested as a potential third cannabinoid receptor. Some cannabinoids, such as anandamide, activate GPR55, however, the only consistent endogenous ligand is LPI, a phospholipid (40). The signaling pathways as well as the structure are also very distinct to those of the cannabinoid receptors. However, I was curious to see what effects could be achieved by modulating the GPR55 activity with an antagonist, CID16020046, that has already been investigated by our group (61). GPR55 is highly expressed in leukocytes, such as lymphocytes, macrophages, neutrophils and platelets (46). $GPR55^{-/-}$ mice exert less inflammation compared to wild-type mice in the DSS model of colitis (49). The GPR55 antagonist CID16020046 has previously been characterized by our group and has shown significant in vitro effects on platelet function by completely reversing LPI-inhibited aggregation (61).

The intestinal epithelium acts as a physical barrier against microbes and metabolic factors of the colon. The turnover of these cells is high (every 3-5-days) and is closely dependent on regulation of proliferation and apoptosis (114). Dextrane sulphate sodium (DSS) is a physical agent that disrupts that epithelial cell barrier, allowing the microbes and their metabolic products to activate mucosal macrophages to produce inflammatory cytokines (7,115,116). It is the concentration of the administered DSS, but not the total amount that is responsible for the extent of colonic damage, which is why minor differences in DSS consumption between animal do not affect the severity of the colonic injury (117). The DSS-induced experimental model of colitis is a predominantly macrophage-driven model of experimental colitis (117). The regeneration in this colitis model is rather slow because DSS is toxic to the basal crypts, causing a full destruction of the crypts. Therefore, the regeneration has to start from the adjacent crypts to produce a bridge over large focal defects. Another possible explanation for the slow regeneration process is also the impaired phagocytosis of macrophages that are saturated with DSS (118). During active DSS colitis, the basal part of the lamina propria were shown to have significantly higher amounts of CD4+ T cells as compared to healthy animals (117). In the trinitrobenzene sulfonic acid (TNBS) colitis model, the colitis is induced by haptenation of colonic proteins (119). This further causes a hypersensitivity reaction caused by CD4+ helper (Th1) reaction to self-antigens. This course of the disease resembles Crohn´s disease in human (120). Our experiments revealed that inhibition of GPR55 with the antagonist as well as the genetic deletion of GPR55 protected against both DSS- and TNBS-induced colitis macroscopically and microscopically. MPO activity, as an inflammation marker, was also reduced in both colitis models, indicating a proinflammatory role of GPR55 in experimental colitis.

In our experiments we saw a decrease of COX-2 and that coincided with an improvement of the inflammation. The decrease seen in the colitis models may be helpful for healing, however the role of COX-2 in the inflammatory process is still not clear. Severity of DSS-induced colitis was shown to be exacerbated when COX-2 was inhibited at the early stage of DSS exposure, therefore, NSAIDs may

be able to exacerbate the inflammatory response in UC patients (81). In other studies of DSS colitis, it was suggested that selective COX-2 inhibition by Rofecoxib treatment improved DSS colitis most probably by reducing neutrophil infiltration, decreasing IL-1β expression and normalizing COX-1 expression levels in the inflamed mucosa, suggesting that COX-2 does not contribute to the observed protective effect (121). NSAIDs that non-selectively inhibit both COX-1 and COX-2 isoforms cause damage to the intestinal mucosa and promote inflammation, also they cause gastrointestinal bleeding and increase the risk of myocardial infarction (100,122). Despite the clinical evidence that selective COX-2 inhibitors have less GI side effects, it has been argued that COX-2 might also be responsible for the production of prostaglandins that are involved in the healing process of ulcers (123,124).

Cytokines are important mediators of the immune system (12). IL-1β was the only cytokine that was significantly reduced in both the DSS and TNBS colitis models in the CID1020046 treated group of mice. TNF-α was only reduced in the DSS model, however, a tendency towards the decrease in the CID16020046 treated group was also observed in the TNBS model. IL-6 appears to have different effects in these two experimental colitis models, being reduced in the TNBS model but unaltered in the DSS model. TNF-α has been shown to be involved in the pathogenesis of various inflammatory diseases, for instance rheumatoid arthritis, multiple sclerosis and IBD (125). During the active phase of IBD, in human (126) as well as in experimental mouse models (127,128), tumor necrosis factor receptor 2 (TNF-R2) expression is increased (127). Interestingly, in humans, polymorphisms of the TNF-R2 gene have been connected to a higher susceptibility to Crohn's disease (126). IL-1β is responsible for recruitment of inflammatory cells to the site of bacterial infection (129). Treatment of DSS-exposed mice with a IL-1β antibody weakened the severity of the disease (130). Although the use of TNF-α as an inflammation marker and the use of TNF-α antibodies in the treatment of ulcerative colitis is widespread, the precise role of TNF-α in colitis is not fully understood. In the TNBS model, an infiltration of inflammatory cells into all layers of the is characteristic (131). Whilst the survival

rate of TNF-$\alpha^{-/-}$ knockout mice in a DSS model was lower than that of TNF-$\alpha^{+/+}$ wild types, in the TNBS model TNF-$\alpha^{-/-}$ knockouts do not even develop disease after being challenged with TNBS (132,120). While TNFR1$^{-/-}$ mice (that have a deletion of TNF α receptor1) survive lethal doses of LPS, in the TNBS colitis model, TNFR1$^{-/-}$ mice had a worse clinical course of disease compared to TNFR2$^{-/-}$ mice (133).

TNF-α can interact with two different soluble forms of TNF receptors, the p55 and p75 form. Both forms inhibit the binding of TNF to cellular receptors, thereby diminishing its biologic effects (134). TNFR1 contains a death domain that mediates apoptosis and further downstream activation of NFκB through caspase activation. TNFR2 does not have a death domain but is still capable to activate apoptosis through the kinase receptor interacting protein (RIP) (120). It is, however, not clear if differences like these were responsible that we had no significant reduction in the TNBS colitis after application of the GPR55 inhibitor.

IL-6 has a role in supporting hematopoiesis, modulating immune responses and regulation of acute phase reactions (135). It acts primarily on protecting the mucosal surface against infection-induced epithelial ulceration (136). It was also suggested that STAT3 inhibition in vivo and in vitro leads to tumor cell apoptosis and inhibition of growth (137). The IL-6/STAT3 signaling has been suggested to influence the development of disease severity (138,139). The IL-6 receptor consists of a IL-6 specific binding unit, an α chain and a signal-transduction unit gp130 (135). CD4+ T cells have the gp130 expressed on their membranes that interact with the IL-6-sIL-6R complexes (138). Further downstream signaling pathways cause induction of antiapoptotic genes as for instance Bcl-2 and Bcl-xL, causing resistance of lamina propria T cells to apoptosis. Accumulation of T cells and resistance to apoptosis then lead to chronic inflammation (6). But IL-6 has also a tissue-protective role in the gastrointestinal mucosa where it is involved in mucosal regeneration after injury (18). STAT1- and STAT 3-activation is observed in inflamed tissues of UC and CD patients, and STAT3 is found to strongly correlate to the severity of inflammation (140). IL-6 is consistently elevated in IBD

tissues, and next to macrophages can also be produced by epithelial cells (10). Crohn's disease patients have elevated IL-6 levels in the blood, whilst this effect was not observed in UC patients (141).

Due to the described differences of various cytokines in these two experimental colitis models, it might be that in the TNBS model IL-6 acts more as a proinflammatory cytokine, whilst in the DSS model it acts on mucosal regeneration. Also, the time points of regeneration to set in differ in these two colitis models, which might also explain differences in the expression between IL-6 and STAT3. Either way, the macroscopic outcome is the same: the CID16020046 group had a significantly less severe colitis compared to the vehicle groups. Similarly, the CID16020046-induced COX-2 reduction observed in both models went hand in hand with improved scores.

Due to the differences in IL-6 levels observed in the two models, I was interested if levels of phosphorylated STAT3 (pSTAT3) were also different. Indeed, in the DSS model, in which IL-6 levels were unaltered as compared to the vehicle group, pSTAT3 levels were significantly reduced, while in the TNBS model, in which IL-6 levels were significantly decreased in the GPR55 antagonist-treated group, pSTAT3 levels were significantly increased. It would be interesting to investigate the IL-6/STAT3 signaling in more detail to find out what exact mechanism contributes to the different effects, whether they are due to the different courses of the diseases or due to different onsets of mucosal restitution. About 70% of all lymphocytes are located in the mucosal immune system of the gut (142), and about 10% of all lamina propria mononuclear cells are macrophages (143). Leukocyte recruitment into the mucosa is characteristic for the active disease phase (10,144). Patients who suffer from UC or CD have a constant overproduction of monocytes, probably due to an increased demand of macrophages in the inflamed mucosa (10). Macrophages and neutrophils are the first to invade the inflamed mucosa, and thereby contribute significantly to the pathogenesis of the disease because they produce a wide variety of inflammatory mediators such as TNF-α, IL-1β, IL-6 and reactive oxygen species (14,116,145).

They also present antigens to T lymphocytes (146). It is known that the number of macrophages increases during the course of colitis, this is in agreement with our observation of a significant increase of macrophages at the end of the experiment. Besides, macrophages are able to phagocytose DSS (147). CID16020046 caused reduction of lymphocyte recruitment, measured by CD3 staining, into the lamina propria in both the DSS and TNBS model. Macrophage influx was also diminished in the DSS model in CID16020046 treated animals, which was also confirmed by the immunohistological staining. Interestingly, the number of recruited neutrophils in CID16020046 treated mice was increased, which seems contradictory to the observed reduction of MPO activity in CID16020046 treated mice. It should be mentioned that cannabidiol, which inhibits GPR55 activity (41,148) was shown to inhibit MPO activity in neutrophils (149). This also could have been the case for CID16020046.

Neutrophils activation and accumulation is one of the crucial pathological features of active IBD. Neutrophils significantly contribute to the development of the disease and their depletion was shown to be protective for the development of the disease although there are also reports stating the contrary, that neutrophil depletion might worsen the course of the disease (150,151). In human neutrophils, GPR55 has been shown to increase migratory responses of CB2 to 2-AG. This interesting finding might suggest a possibility of an interaction between the cannabinoid receptors and GPR55 (48). Also we found that neutrophils slowed in their migration after incubation with CID which is in perfect agreement with the finding by Balenga et al. that GPR55 activation induces migration in neutrophils (47).

In the mouse macrophage cell line J774.1, CID160020046 was able to reduce transwell migration to C5a and MCP-1-induced expression of CD11b, a marker that is increased in the inflamed colonic mucosa (152). This indicates that the effect of reduced macrophage recruitment into the lamina propria might be due to a direct impact of CID16020046 on macrophages.

4.2. Part 2 - Pharmacological and genetic inhibition of MAGL in experimental colitis and colitis-associated colon cancer: Role of 2-AG

Current treatment of IBD includes the use of glucocorticoids. They affect monocyte chemotaxis, reduce the production of prostaglandins, monokines and leukotrienes, as well as inhibit T cell proliferation and differentiation of B cells (12). Also, 5-aminosalicylic acid drugs are standard therapeutics for relieving IBD symptoms. They act by inhibiting cyclooxygenase, lipoxygenase and thromboxane synthesis (153). As COX-2 expression is heightened in certain cancers, non-steroidal anti-inflammatory drugs (NSAIDs) have been shown to reduce the risk of carcinogenesis of breast, colon, lung and prostate cancer by inhibiting COX activity, (154,155). However, the safe use of NSAIDs in IBD is still unclear (156). Besides, the use of all of those pharmacological agents has side effects and is not an optimal treatment solution (14).

The effects of cannabinoids in intestinal inflammation have been known for quite some time now. They have been well studied revealing that both cannabinoid receptors play a role in the pathogenesis of experimental colitis (39). Both cannabinoid receptors have been shown to be protective in models of experimental colitis (87,123). Monoacylglycerol lipase is the main enzyme responsible for degrading 2-AG, which is a full agonist of both cannabinoid receptors (91). Therefore, it has been thought that raising 2-AG levels through inhibition of MAGL, should have protective effects on the development of experimental colitis (102). Recently, it was shown that $MAGL^{-/-}$ mice have high 2-AG expression in the colon as compared to other parts of the intestinal tract, namely the duodenum, jejunum and ileum (71). The inhibition of intracellular degradation of 2-AG has been shown to be protective against intestinal inflammation (91). Both the genetic and pharmacological inhibition of MAGL showed macroscopic improvement of DSS-induced colitis. I was curious to see

whether the observed improvement could also be seen at the molecular base, and I therefore measured COX-2 expression in colon samples of JZL184-treated and vehicle-treated mice with colitis, as well as IL-6 and IL-1β, two cytokines that have been shown to be involved in the pathology of IBD (81). JZL184 treatment was shown to raise 2-AG levels at the dosage of 40mg/kg (82). At the dosage I used, 32mg/kg, it was able to significantly inhibit COX-2 expression and showed a strong tendency towards decrease of IL-6 and IL-1β levels. The improvement of colitis was also visible in $MAGL^{-/-}$ mice, showing crypt architecture that is much better preserved than in the wild-type mice.

MAGL, being the enzyme responsible for 2-AG degradation, could also provide a pool of arachidonic acid that is the substrate for COX enzymes, and as COX products may influence colon carcinogenesis (154), I wondered what effect MAGL inhibition could have on tumor development in a model of AOM-DSS induced colon cancer. The model of DSS+azoxymethane (AOM) colitis-associated cancer is well established and widely used. AOM is used to increase the incidence of tumors, because when mice are administered only DSS, tumors develop only in 15-20% (157). My experiments showed that low dose of JZL184 administered in weeks 8-10 did decrease total tumor size, whilst JZL184 treatment at earlier time points at different dosages did not show any effect on tumor size compared to the vehicle treated animals suggesting inhibition of tumor growth later in the development.

In a TNBS-induced colitis model, JZL184 treatment reduced macroscopic and histological colon alterations and it also restored the integrity of the intestinal barrier function (91). When JZL184 was applied in a model of pain at a low dose (8mg/kg) for 6 days, anti-allodynic and anti-edematous effects were maintained, but after prolonged inactivation of MAGL with a high dose of JZL184 (40mg/kg, 6 days) caused CB1 receptor downregulation and desensitization in several brain regions such as cingulated cortex, hippocampus, somatosensory cortex and peraqueductal grey was observed. Through application of specific antagonists, the authors of the study found that the anti-allodynic effects were CB1-mediated and

the anti-edematous were CB2 mediated (27). In another study, $MAGL^{-/-}$ knockout mice also showed partial desensitization of CB1 receptors (67). Such effects were not observed when FAAH was inhibited by PF-3845. It was shown that sustained elevations in 2-AG levels of the brain caused functional antagonism and disruptions in endocannabinoid-dependent synaptic plasticity. Also, JZL184 treatment caused a more pronounced cross-tolerance to CB1 than the genetic disruption of MAGL (67). In a recent paper (102), Taschler and coworkers could show that CB1 receptors are desensitized in the intestine of $MAGL^{-/-}$ knockout mice suggesting that the lower tumorigenesis in $MAGL^{-/-}$ mice observed in our experiments does not include CB1 activity. This is of particular interest as deletion of the CB1 receptor in APC $^{min/+}$ accelerates intestinal tumorigenesis (158) therefore, presence of the CB1 receptor in the gut likely protects against tumorigenesis. Thus, the ameliorating effect of MAGL inhibition on cancer growth seen in our experiments likely uses non-CB1 mediated pathways. Thus, for instance, less arachidonic acid could have been produced, thereby causing a reduction in inflammatory and protumorigenic mediator production.

Since I administered JZL184 for more than 10 days, which was shown in a different study to be enough to cause cross-tolerance and CB1 receptor desensitization (63). Hence, a possible explanation could be that CB1 receptors were desensitized and therefore the protective effect of MAGL inhibition by JZL184 was blunted. Interestingly, when JZL184 was given at a later time point and a lower dosage was administered, JZL184 in fact did cause a significant total tumor area reduction, indicating that pharmacological MAGL inhibition in an inflammation-driven colon cancer model might not lead to CB1 desensitization. MAGL inhibition seems to have a greater effect on tumor promotion than on tumor initiation. $MAGL^{-/-}$ mice showed decreased total tumor area compared to wild type mice. MAGL inactivation has also been shown to have a protective role in colitis (91). Interestingly, another study showed that in human cancers (breast, lung and ovary) MAGL expression was reduced or lost, and exogenous expression of MAGL in tumor cells lacking this enzyme suppressed their growth (159). Other studies however, showed that in aggressive cancer cells, MAGL provides free fatty

acids that are needed for the production of protumorigenic signaling lipids (79). Nonaggressive cancer cell lines became aggressive and invasive when MAGL was overexpressed. Therefore, MAGL has been suggested to be both sufficient and necessary (both aggressive and nonaggressive cancer cells exhibited similar levels of fatty acid synthase; FAS) to elevate free fatty acid content and thereby increase migratory and tumorigenic activity in cancer cells (79,84,160). Interestingly, it was shown that MAGL blockade protected gastrointestinal bleeding that was caused by diclofenac (a dual COX-1/COX-2 inhibitor), through CB1 receptor (161). When applied alone, JZL184 did not cause gastric hemorrhaging that was observed in either COX-1 or COX1/COX-2 inhibitors (86). Anandamide and 2-AG content was shown to increase during colon carcinogenesis when passing from normal mucosa to adenomatous polyps, and then again the levels slightly decreased in the colorectal cancer tissue. Levels of anandamide were enough in the adenomatous polyps to activate CB1 receptors, and 2-AG levels were sufficient even in the healthy mucosa, but it has to be kept in mind that probably not all the 2-AG may be used as an endocannabinoid. 2-AG is only partially released outside the cells to activate the cannabinoid receptors, as it is also involved in the (phospho)glyceride metabolism (38). Applying 2-AG exogenously was shown to reduce NFκB phosphorylation and COX-2 expression, but was also shown to increase the invasion of prostate cancer cells, presumably due to increased arachidonic acid (AA) levels (162,163). In vitro studies have shown that LPS stimulations cause anandamide and 2-AG production by immune cells, including macrophages (164).

In our AOM+DSS experiments, total tumor area was reduced in the two models of pharmacological and genetic inhibition of MAGL. Inhibition of MAGL also showed a strong tendency to decrease total tumor area in the spontaneous model of colon cancer indicating a protumorigenic role of MAGL even in the spontaneous cancer model, where the inflammatory drive of DSS was not present. MAGL might indeed provide free fatty acids that are needed for building new membranes of tumor cells, that way driving carcinogenesis. This suggests that the anti-tumorigenic effect of MAGL inhibition could be due to a decreased pool of free fatty acids and

a smaller pool of arachidonic acid than through enhanced cannabinoid signaling. However, this remains speculative, as arachidonic acid and free fatty acid levels were not measured in our experiments. Further experiments are necessary to investigate whether these speculations may hold true.

In conclusion, I could demonstrate that the novel GPR55 inhibitor CID1602004 was protective in two models of experimental IBD by interfering with lymphocyte and macrophage recruitment to the colon. The GPR55 inhibitor exerted direct effects on the mouse macrophage cell line J774.1 by reducing migration and CD11b activation. GPR55 has therefore functions different to CB receptors in bowel inflammation, which are primarily antiinflammatory. Since GPR55 is responsive to cannabinoids, it may represent an important modulator of CB receptor actions during bowel inflammation and an interesting drug target. I further showed that MAGL knockout mice, which express high levels of the endocannabinoid 2-AG, were protected against intestinal inflammation and colitis-associated cancer. This is of particular interest because it was shown that CB1 receptors in the gut of MAGL knockout mice are desensitized and an antiinflammatory/anticarcinogenic effect of 2-AG is therefore not likely. Future experiments will hopefully reveal the non-CB1 receptor pathways by which 2-AG may act as an antiinflammatory/anticarcinogenic mediator.

References

1. Xavier RJ, Podolsky DK. Unravelling the pathogenesis of inflammatory bowel disease. Nature. 2007 Jul;448(7152):427–34.

2. Baumgart DC, Sandborn WJ. Inflammatory bowel disease: clinical aspects and established and evolving therapies. Lancet. 2007 May;369(9573):1641–57.

3. Baumgart DC, Carding SR. Inflammatory bowel disease: cause and immunobiology. Lancet. 2007 May;369(9573):1627–40.

4. Fichtner-feigl S, Fuss IJ, Preiss JC, Strober W, Kitani A. Treatment of murine Th1- and Th2-mediated inflammatory bowel disease with NF- κ B decoy oligonucleotides. J Clin Invest. 2005 Nov;115(11):3057–71.

5. Schwartz DA, Pemberton JH, Sandborn WJ. Diagnosis and treatment of perianal fistulas in Crohn disease. Ann Intern Med. 2001 Nov;135(10):906–18.

6. Jiang H-R, Gilchrist DS, Popoff J-F, Jamieson SE, Truscott M, White JK, et al. Influence of Slc11a1 (formerly Nramp1) on DSS-induced colitis in mice. J Leukoc Biol. 2009 Apr;85(4):703–10.

7. Alex P, Zachos NC, Nguyen T, Gonzales L, Chen TE, Conklin LS, et al. Distinct cytokine patterns identified from multiplex profiles of murine DSS and TNBS-induced colitis. Inflamm Bowel Dis. 2010;15(3):341–52.

8. Blumberg RS, Saubermann LJ, Strober W. Animal models of mucosal inflammation and their relation to human inflammatory bowel disease. Curr Opin Immunol. 1999 Dec;11(6):648–56.

9. Ma X, Torbenson M, Hamad a R a, Soloski MJ, Li Z. High-fat diet modulates non-CD1d-restricted natural killer T cells and regulatory T cells in mouse

colon and exacerbates experimental colitis. Clin Exp Immunol. 2008 Jan;151(1):130–8.

10. Fiocchi C. Inflammatory bowel disease: Etiology and pathogenesis. Gastroenterology. 1998 Jul;115(1):182–205.

11. Strober W, Fuss I, Mannon P. The fundamental basis of inflammatory bowel disease. J Clin Invest. 2007 Mar;117(3):514–21.

12. Kołodziejska-Sawerska a, Rychlik a, Depta a, Wdowiak M, Nowicki M, Kander M. Cytokines in canine inflammatory bowel disease. Pol J Vet Sci. 2013 Jan;16(1):165–71.

13. Sanchez-Muñoz F, Dominguez-Lopez A, Yamamoto-Furusho JK. Role of cytokines in inflammatory bowel disease. World J Gastroenterol. 2008 Jul;14(27):4280–8.

14. Islam MS, Murata T, Fujisawa M, Nagasaka R, Ushio H, Bari a M, et al. Anti-inflammatory effects of phytosteryl ferulates in colitis induced by dextran sulphate sodium in mice. Br J Pharmacol. 2008 Jun;154(4):812–24.

15. Ravikoff Allegretti J, Courtwright A, Lucci M, Korzenik JR, Levine J. Marijuana use patterns among patients with inflammatory bowel disease. Inflamm Bowel Dis. 2013 Dec;19(13):2809–14.

16. Schicho R, Storr M. IBD patients find symptom relief in the Cannabis field. Nat Rev Gastroenterol Hepatol. 2014 Mar;11(3):142–3.

17. Naftali T, Bar-Lev Schleider L, Dotan I, Lansky EP, Sklerovsky Benjaminov F, Konikoff FM. Cannabis induces a clinical response in patients with Crohn's disease: a prospective placebo-controlled study. Clin Gastroenterol Hepatol. 2013 Oct;11(10):1276–80.e1.

18. Terzić J, Grivennikov S, Karin E, Karin M. Inflammation and colon cancer. Gastroenterology. 2010 Jun;138(6):2101–14.e5.

19. Grivennikov S, Karin E, Terzic J, Mucida D, Yu G-Y, Vallabhapurapu S, et al. IL-6 and Stat3 are required for survival of intestinal epithelial cells and development of colitis-associated cancer. Cancer Cell. 2009 Feb;15(2):103–13.

20. Karin M, Greten FR. NF-kappaB: linking inflammation and immunity to cancer development and progression. Nat Rev Immunol. 2005 Oct;5(10):749–59.

21. Sheng H, Shao J, Williams CS, Pereira MA, Taketo MM, Oshima M, et al. Nuclear translocation of beta-catenin in hereditary and carcinogen-induced intestinal adenomas. Carcinogenesis. 1998 Apr;19(4):543–9.

22. Alexander A, Smith PF, Rosengren RJ. Cannabinoids in the treatment of cancer. Cancer Lett. 2009 Nov;285(1):6–12.

23. Mulvihill MM, Nomura DK. Therapeutic potential of monoacylglycerol lipase inhibitors. Life Sci. 2013 Mar;92(8-9):492–7.

24. Izzo A a, Sharkey K a. Cannabinoids and the gut: new developments and emerging concepts. Pharmacol Ther. 2010 Apr;126(1):21–38.

25. Gustafsson SB, Lindgren T, Jonsson M, Jacobsson SOP. Cannabinoid receptor-independent cytotoxic effects of cannabinoids in human colorectal carcinoma cells: synergism with 5-fluorouracil. Cancer Chemother Pharmacol. 2009 Mar;63(4):691–701.

26. DeMorrow S, Glaser S, Francis H, Venter J, Vaculin B, Vaculin S, et al. Opposing actions of endocannabinoids on cholangiocarcinoma growth: recruitment of Fas and Fas ligand to lipid rafts. J Biol Chem. 2007 Apr;282(17):13098–113.

27. Ghosh S, Wise LE, Chen Y, Gujjar R, Mahadevan A, Cravatt BF, et al. The monoacylglycerol lipase inhibitor JZL184 suppresses inflammatory pain in the mouse carrageenan model. Life Sci. 2013 Mar;92(8-9):498–505.

28. Ueda N, Tsuboi K. Discrimination between two endocannabinoids. Chem Biol. 2012 May;19(5):545–7.

29. Fonseca BM, Costa M a, Almada M, Correia-da-Silva G, Teixeira N a. Endogenous cannabinoids revisited: a biochemistry perspective. Prostaglandins Other Lipid Mediat. 2013 Apr-May;102-103(228):13–30.

30. Ross R a. The enigmatic pharmacology of GPR55. Trends Pharmacol Sci. 2009 Mar;30(3):156–63.

31. Schicho R, Storr M. Targeting the endocannabinoid system for gastrointestinal diseases: future therapeutic strategies. Expert Rev Clin Pharmacol. 2010 Mar;3(2):193–207.

32. Engeli S, Böhnke J, Feldpausch M, Gorzelniak K, Janke J, Bátkai S, et al. Activation of the peripheral endocannabinoid system in human obiesity. Diabetes. 2005 Oct;54(10):2838–43.

33. Wright KL, Duncan M, Sharkey KA. Cannabinoid CB2 receptors in the gastrointestinal tract: a regulatory system in states of inflammation. Br J Pharmacol. 2008 Jan;153(2):263–70.

34. Storr M, Gaffal E, Saur D, Schusdziarra V, Allescher HD. Effect of cannabinoids on neural transmission in rat gastric fundus. Can J Physiol Pharmacol. 2002 Jan;80(1):67–76.

35. Van Gaal L, Pi-Sunyer X, Despres J-P, McCarthy C, Scheen A. Efficacy and safety of rimonabant for improvement of multiple cardiometabolic risk factors in overweight/obese patients: pooled 1-year data from the Rimonabant in Obesity (RIO) program. Diabetes Care. 2008 Feb;31 Suppl 2:S229–40.

36. Glass M, Northup JK. Agonist selective regulation of G proteins by cannabinoid CB(1) and CB(2) receptors. Mol Pharmacol. 1999 Dec;56(6):1362–9.

37. Brown I, Cascio MG, Rotondo D, Pertwee RG, Heys SD, Wahle KWJ. Cannabinoids and omega-3/6 endocannabinoids as cell death and anticancer modulators. Prog Lipid Res. 2013 Jan;52(1):80–109.

38. Ligresti A, Bisogno T, Matias I, De Petrocellis L, Cascio MG, Cosenza V, et al. Possible endocannabinoid control of colorectal cancer growth. Gastroenterology. 2003 Sep;125(3):677–87.

39. Izzo AA, Camilleri M. Cannabinoids in intestinal inflammation and cancer. Pharmacol Res. 2009 Aug;60(2):117–25.

40. Howlett AC. Efficacy in CB1 receptor-mediated signal transduction. Br J Pharmacol. 2004 Aug;142(8):1209–18.

41. Ryberg E, Larsson N, Sjögren S, Hjorth S, Hermansson N-O, Leonova J, et al. The orphan receptor GPR55 is a novel cannabinoid receptor. Br J Pharmacol. 2007 Dec;152(7):1092–101.

42. Sharir H, Abood ME. Pharmacological characterization of GPR55, a putative cannabinoid receptor. Pharmacol Ther. 2010 Jun;126(3):301–13.

43. Henstridge CM, Balenga N a B, Ford L a, Ross R a, Waldhoer M, Irving AJ. The GPR55 ligand L-alpha-lysophosphatidylinositol promotes RhoA-dependent Ca2+ signaling and NFAT activation. FASEB J. 2009 Jan;23(1):183–93.

44. Henstridge CM. Off-target cannabinoid effects mediated by GPR55. Pharmacology. 2012 Jan;89(3-4):179–87.

45. Sawzdargo M, Nguyen T, Lee DK, Lynch KR, Cheng R, Heng HH, et al. Identification and cloning of three novel human G protein-coupled receptor genes GPR52, PsiGPR53 and GPR55: GPR55 is extensively expressed in human brain. Brain Res Mol Brain Res. 1999 Feb;64(2):193–8.

46. Henstridge CM, Balenga N a B, Kargl J, Andradas C, Brown AJ, Irving A, et al. Minireview: recent developments in the physiology and pathology of the lysophosphatidylinositol-sensitive receptor GPR55. Mol Endocrinol. 2011 Nov;25(11):1835–48.

47. Balenga N a B, Aflaki E, Kargl J, Platzer W, Schröder R, Blättermann S, et al. GPR55 regulates cannabinoid 2 receptor-mediated responses in human neutrophils. Cell Res. 2011 Oct; 21(10):1452–69.

48. Schicho R, Storr M. A potential role for GPR55 in gastrointestinal functions. Curr Opin Pharmacol. 2012 Dec;12(6):653–8.

49. Schicho R, Bashashati M, Bawa M, McHugh D, Saur D, Hu H-M, et al. The atypical cannabinoid O-1602 protects against experimental colitis and inhibits neutrophil recruitment. Inflamm Bowel Dis. 2011 Aug;17(8):1651–64.

50. Lauckner JE, Jensen JB, Chen H-Y, Lu H-C, Hille B, Mackie K. GPR55 is a cannabinoid receptor that increases intracellular calcium and inhibits M current. Proc Natl Acad Sci U S A. 2008 Feb;105(7):2699–704.

51. Kargl J, Balenga N, Parzmair GP, Brown AJ, Heinemann A, Waldhoer M. The cannabinoid receptor CB1 modulates the signaling properties of the lysophosphatidylinositol receptor GPR55. J Biol Chem. 2012 Dec;287(53):44234–48.

52. Oka S, Nakajima K, Yamashita A, Kishimoto S, Sugiura T. Identification of GPR55 as a lysophosphatidylinositol receptor. Biochem Biophys Res Commun. 2007 Nov;362(4):928–34.

53. Kotsikorou E, Madrigal KE, Hurst DP, Sharir H, Lynch DL, Heynen-genel S, et al. Identification of the GPR55 agonist binding site using a novel set of high-potency GPR55 selective ligands. Biochemistry. 2011 Jun;50(25):5633–47.

54. Anavi-Goffer S, Baillie G, Irving AJ, Gertsch J, Greig IR, Pertwee RG, et al. Modulation of L-alpha-lysophosphatidylinositol/GPR55 mitogen-activated protein kinase (MAPK) signaling by cannabinoids. J Biol Chem. 2012 Jan;287(1):91–104.

55. Simcocks AC, O'Keefe L, Jenkin K a, Mathai ML, Hryciw DH, McAinch AJ. A potential role for GPR55 in the regulation of energy homeostasis. Drug Discov Today. 2014 Aug;19(8):1145-51.

56. Staton PC, Hatcher JP, Walker DJ, Morrison AD, Shapland EM, Hughes JP, et al. The putative cannabinoid receptor GPR55 plays a role in mechanical hyperalgesia associated with inflammatory and neuropathic pain. Pain. 2008 Sep;139(1):225–36.

57. Lin X-H, Yuece B, Li Y-Y, Feng Y-J, Feng J-Y, Yu L-Y, et al. A novel CB receptor GPR55 and its ligands are involved in regulation of gut movement in rodents. Neurogastroenterol Motil. 2011 Sep;23(9):862–e342.

58. Schicho R, Storr M. Topical and systemic cannabidiol improves trinitrobenzene sulfonic acid colitis in mice. Pharmacology. 2012 Jan;89(3-4):149–55.

59. Balenga N a, Martínez-Pinilla E, Kargl J, Schröder R, Peinhaupt M, Platzer W, et al. Heteromerization of GPR55 and cannabinoid CB2 receptors modulates signalling. Br J Pharmacol. 2014 Jul;171(23):5387-406.

60. Moreno E, Andradas C, Medrano M, Caffarel MM, Pérez-Gómez E, Blasco-Benito S, et al. Targeting CB2-GPR55 receptor heteromers modulates cancer cell signaling. J Biol Chem. 2014 Aug;289(32):21960–72.

61. Kargl J, Brown AJ, Andersen L, Dorn G, Schicho R, Waldhoer M, et al. A Selective Antagonist Reveals a Potential Role of G Protein-Coupled Receptor 55 in Platelet and Endothelial Cell Function. J Pharmacol Exp Ther. 2013 Jul;346(1):54–66.

62. Di Marzo V, Fontana A, Cadas H, Schinelli S, Cimino G, Schwartz JC, et al. Formation and inactivation of endogenous cannabinoid anandamide in central neurons. Nature. 1994 Dec;372(6507):686–91.

63. Marzo V Di, Toiano V, Felice A. ` Endocannabinoids ' and other fatty acid derivatives with cannabimimetic properties : biochemistry and possible physiopathological relevance. Biochim Biophys acta. 1998 Jun;1392(2-3):153-75.

64. Banni S, Di Marzo V. Effect of dietary fat on endocannabinoids and related mediators: consequences on energy homeostasis, inflammation and mood. Mol Nutr Food Res. 2010 Jan;54(1):82–92.

65. Di Marzo V. A brief history of cannabinoid and endocannabinoid pharmacology as inspired by the work of British scientists. Trends Pharmacol Sci. 2006 Mar;27(3):134–40.

66. Ahn K, McKinney MK, Cravatt BF. Enzymatic pathways that regulate endocannabinoid signaling in the nervous system. Chem Rev. 2008 May;108(5):1687–707.

67. Schlosburg JE, Blankman JL, Long JZ, Nomura DK, Pan B, Kinsey SG, et al. Chronic monoacylglycerol lipase blockade causes functional antagonism of the endocannabinoid system. Nat Neurosci. 2010 Sep;13(9):1113–9.

68. Yates ML, Barker EL. Inactivation and biotransformation of the endogenous cannabinoids anandamide and 2-arachidonoylglycerol. Mol Pharmacol. 2009 Jul;76(1):11–7.

69. Duncan M, Thomas AD, Cluny NL, Patel A, Patel KD, Lutz B, et al. Distribution and function of monoacylglycerol lipase in the gastrointestinal tract. Am J Physiol Gastrointest Live Physiol. 2008 Dec;295(6):1255–65.

70. Pinto L, Izzo AA, Cascio MG, Bisogno T, Hospodar-Scott K, Brown DR, et al. Endocannabinoids as physiological regulators of colonic propulsion in mice. Gastroenterology. 2002 Jul;123(1):227–34.

71. Taschler U, Eichmann TO, Radner FP, Wolinski H, Storr M, Lass A, Schicho R, Zimmermann R. Monoglyceride lipase-deficiency causes desensitization of intestinal cannabinoid 1 receptors and increased colonic μ-opiod sensitivity. Br J Pharmacol. Manuscript submitted for publication.

72. Turcotte C, Chouinard F, Lefebvre JS, Flamand N. Regulation of inflammation by cannabinoids, the endocannabinoids 2-arachidonoyl-glycerol and arachidonoyl-ethanolamide, and their metabolites. J Leukoc Biol. 2015 Jun;97(6):1049–70.

73. Saario SM, Laitinen JT. Therapeutic potential of endocannabinoid-hydrolysing enzyme inhibitors. Basic Clin Pharmacol Toxicol. 2007 Nov;101(5):287–93.

74. Eijkelkamp N, Heijnen CJ, Lucas A, Premont RT, Elsenbruch S, Schedlowski M, et al. G protein-coupled receptor kinase 6 controls chronicity and severity of dextran sodium sulphate-induced colitis in mice. Gut. 2007 Jun;56(6):847–54.

75. Gulyas AI, Cravatt BF, Bracey MH, Dinh TP, Piomelli D, Boscia F, et al. Segregation of two endocannabinoid-hydrolyzing enzymes into pre- and postsynaptic compartments in the rat hippocampus, cerebellum and amygdala. Eur J Neurosci. 2004 Jul;20(2):441–58.

76. Blankman JL, Simon GM, Cravatt BF. A comprehensive profile of brain enzymes that hydrolyze the endocannabinoid 2-arachidonoylglycerol. Chem Biol. 2007 Dec;14(12):1347–56.

77. Kim J, Alger BE. Inhibition of cyclooxygenase-2 potentiates retrograde endocannabinoid effects in hippocampus. Nat Neurosci. 2004 Jul;7(7):697–8.

78. Labar G, Bauvois C, Borel F, Ferrer J-L, Wouters J, Lambert DM. Crystal structure of the human monoacylglycerol lipase, a key actor in endocannabinoid signaling. Chembiochem. 2010 Jan;11(2):218–27.

79. Nomura DK, Long JZ, Niessen S, Hoover HS, Cravatt BF. Monoacylclycerol lipase regulates a fatty acid network that promotes cancer pathogenesis. Cell. 2010 Jan;140(1):49–61.

80. Wang D, Dubois RN. Eicosanoids and cancer. Nat Rev Cancer. 2010 Mar;10(3):181–93.

81. Hennebert O, Pelissier M-A, Le Mee S, Wülfert E, Morfin R. Anti-inflammatory effects and changes in prostaglandin patterns induced by 7beta-hydroxy-epiandrosterone in rats with colitis. J Steroid Biochem Mol Biol. 2008 Jun;110(3-5):255–62.

82. Long JZ, Li W, Booker L, Burston JJ, Kinsey SG, Schlosburg JE, et al. Selective blockade of 2-arachidonoylglycerol hydrolysis produces cannabinoid behavioral effects. Nat Chem Biol. 2009 Jan;5(1):37–44.

83. Kinsey SG, Long JZ, Cravatt BF, Lichtman AH. Fatty acid amide hydrolase and monoacylglycerol lipase inhibitors produce anti-allodynic effects in mice through distinct cannabinoid receptor mechanisms. J Pain. 2010 Dec;11(12):1420–8.

84. Nomura DK, Long JZ, Niessen S, Hoover HS, Ng S-W, Cravatt BF. Monoacylglycerol lipase regulates a fatty acid network that promotes cancer pathogenesis. Cell. 2010 Jan;140(1):49–61.

85. Fowler CJ. Monoacylglycerol lipase - a target for drug development? Br J Pharmacol. 2012 Jul;166(5):1568–85.

86. Nomura DK, Morrison BE, Blankman JL, Jonathan Z, Kinsey SG, Marcondes MCG, et al. Endocannabinoid hydrolysis generates brain prostaglandins that promote neuroinflammation. Science. 2011 Nov;334(6057):809–13.

87. Massa F, Marsicano G, Hermann H, Cannich A, Monory K, Cravatt BF, et al. The endogenous cannabinoid system protects against colonic inflammation. J Clin Invest. 2004 Apr;113(8):1202–9.

88. Wright K, Rooney N, Feeney M, Tate J, Robertson D, Welham M, et al. Differential expression of cannabinoid receptors in the human colon: cannabinoids promote epithelial wound healing. Gastroenterology. 2005 Aug;129(2):437–53.

89. Malfitano AM, Ciaglia E, Gangemi G, Gazzerro P, Laezza C, Bifulco M. Update on the endocannabinoid system as an anticancer target. Expert Opin Ther Targets. 2011 Mar;15(3):297–308.

90. Klein TW, Cabral GA. Cannabinoid-induced immune suppression and modulation of antigen-presenting cells. J Neuroimmune Pharmacol. 2006 Mar;1(1):50–64.

91. Alhouayek M, Lambert DM, Delzenne NM, Cani PD, Muccioli GG. Increasing endogenous 2-arachidonoylglycerol levels counteracts colitis and related systemic inflammation. FASEB J. 2011 Aug;25(8):2711–21.

92. Izzo AA, Fezza F, Capasso R, Bisogno T, Pinto L, Iuvone T, et al. Cannabinoid CB1-receptor mediated regulation of gastrointestinal motility in mice in a model of intestinal inflammation. Br J Pharmacol. 2001 Oct;134(3):563–70.

93. Izzo A a., Capasso F, Costagliola A, Bisogno T, Marsicano G, Ligresti A, et al. An endogenous cannabinoid tone attenuates cholera toxin-induced fluid accumulation in mice. Gastroenterology. 2003 Sep;125(3):765–74.

94. Esposito I, Proto MC, Gazzerro P, Laezza C, Miele C, Alberobello AT, et al. The Cannabinoid CB1 Receptor Antagonist Rimonabant Stimulates 2-Deoxyglucose Uptake in Skeletal Muscle Cells by Regulating the Expression of Phosphatidylinositol-3-kinase. Mol Pharmacol. 2008 Dec;74(6):1678–86.

95. Ravinet Trillou C, Arnone M, Delgorge C, Gonalons N, Keane P, Maffrand J-P, et al. Anti-obesity effect of SR141716, a CB1 receptor antagonist, in diet-induced obese mice. Am J Physiol Regul Integr Comp Physiol. 2003 Feb;284(2):R345–53.

96. Burdyga G, Lal S, Varro A, Dimaline R, Thompson DG, Dockray GJ. Expression of cannabinoid CB1 receptors by vagal afferent neurons is inhibited by cholecystokinin. J Neurosci. 2004 Mar;24(11):2708–15.

97. Velasco G, Sanchez C, Guzman M. Towards the use of cannabinoids as antitumour agents. Nat Rev Cancer. 2012 Jun;12(6):436–44.

98. Amantini C, Ballarini P, Caprodossi S, Nabissi M, Morelli MB, Lucciarini R, et al. Triggering of transient receptor potential vanilloid type 1 (TRPV1) by capsaicin induces Fas/CD95-mediated apoptosis of urothelial cancer cells in an ATM-dependent manner. Carcinogenesis. 2009 Aug;30(8):1320–9.

99. Greenhough A, Patsos HA, Williams AC, Paraskeva C. The cannabinoid delta(9)-tetrahydrocannabinol inhibits RAS-MAPK and PI3K-AKT survival

signalling and induces BAD-mediated apoptosis in colorectal cancer cells. Int J Cancer. 2007 Nov;121(10):2172–80.

100. Okayama M, Hayashi S, Aoi Y, Nishio H, Kato S, Takeuchi K. Aggravation by selective COX-1 and COX-2 inhibitors of dextran sulfate sodium (DSS)-induced colon lesions in rats. Dig Dis Sci. 2007 Sep;52(9):2095–103.

101. Sina C, Gavrilova O, Förster M, Till A, Derer S, Hildebrand F, et al. G protein-coupled receptor 43 is essential for neutrophil recruitment during intestinal inflammation. J Immunol. 2009 Dec;183(11):7514–22.

102. Taschler U, Radner FPW, Heier C, Schreiber R, Schweiger M, Schoiswohl G, et al. Monoglyceride lipase deficiency in mice impairs lipolysis and attenuates diet-induced insulin resistance. J Biol Chem. 2011 May;286(20):17467–77.

103. Jurjus AR, Khoury NN, Reimund J-M. Animal models of inflammatory bowel disease. J Pharmacol Toxicol Methods. 2004 Oct;50(2):81–92.

104. Scheiffele F, Fuss IJ. Induction of TNBS Colitis in Mice. Curr Protoc Immunol. 2002 Aug; Chapter 15: Unit 15.19.

105. Neufert C, Becker C, Neurath MF. An inducible mouse model of colon carcinogenesis for the analysis of sporadic and inflammation-driven tumor progression. Nat Protoc. 2007;2(8):1998–2004.

106. Farzi A, Reichmann F, Meinitzer A, Mayerhofer R, Jain P, Hassan AM, et al. Synergistic effects of NOD1 or NOD2 and TLR4 activation on mouse sickness behavior in relation to immune and brain activity markers. Brain Behav Immun. 2015 Feb;44:106–20.

107. Sturm EM, Radnai B, Jandl K, Stančić A, Parzmair GP, Högenauer C, et al. Opposing roles of prostaglandin D2 receptors in ulcerative colitis. J Immunol. 2014 Jul;193(2):827–39.

108. Kargl J, Haybaeck J, Stančić A, Andersen L, Marsche G, Heinemann A, et al. O-1602, an atypical cannabinoid, inhibits tumor growth in colitis-associated colon cancer through multiple mechanisms. J Mol Med. 2013 Apr;91(4):449–58.

109. Sakai H, Yamada Y, Shimizu M, Saito K, Moriwaki H, Hara A. Genetic ablation of Tnfalpha demonstrates no detectable suppressive effect on inflammation-related mouse colon tumorigenesis. Chem Biol Interact. 2010 Mar;184(3):423–30.

110. Pfaffl MW. A new mathematical model for relative quantification in real-time RT-PCR. Nucleic Acids Res. 2001 May;29(9):e45.

111. Weigmann B, Tubbe I, Seidel D, Nicolaev A, Becker C, Neurath MF. Isolation and subsequent analysis of murine lamina propria mononuclear cells from colonic tissue. Nat Protoc. 2007 Oct;2(10):2307–11.

112. Wu C-S, Chen H, Sun H, Zhu J, Jew CP, Wager-Miller J, et al. GPR55, a G-protein coupled receptor for lysophosphatidylinositol, plays a role in motor coordination. PLoS One. 2013;8(4):e60314.

113. Li K, Fichna J, Schicho R, Saur D, Bashashati M, Mackie K, et al. A role for O-1602 and G protein-coupled receptor GPR55 in the control of colonic motility in mice. Neuropharmacology. 2013 Aug;71:255–63.

114. Edelblum KL, Washington MK, Koyama T, Robine S, Polk DB. Raf protects against colitis by promoting mouse colon epithelial cell survival through NF-kappaB. Gastroenterology. 2008 Aug;135(2):539–51.

115. Im E, Choi YJ, Pothoulakis C, Rhee SH. Bacillus polyfermenticus Ameliorates Colonic Inflammation by Promoting Cytoprotective Effects in Colitic Mice. J Nutr. 2009 Oct; 139(10):1848-54.

116. Ito R, Shin-Ya M, Kishida T, Urano a, Takada R, Sakagami J, et al. Interferon-gamma is causatively involved in experimental inflammatory bowel disease in mice. Clin Exp Immunol. 2006 Nov;146(2):330–8.

117. Egger B, Thomas B, Macdonald T. Original Paper : Inflammatory Bowel Disease Characterisation of Acute Murine Dextran Sodium Sulphate Colitis: Cytokine Profile and Dose Dependency. Digestion. 2000;62(4):240–8.

118. Dieleman L a, Palmen MJ, Akol H, Bloemena E, Peña a S, Meuwissen SG, et al. Chronic experimental colitis induced by dextran sulphate sodium (DSS) is characterized by Th1 and Th2 cytokines. Clin Exp Immunol. 1998 Dec;114(3):385–91.

119. Wirtz S, Neufert C, Weigmann B, Neurath MF. Chemically induced mouse models of intestinal inflammation. Nat Protoc. 2007;2(3):541–6.

120. Ebach DR, Newberry R, Stenson WF. Differential role of tumor necrosis factor receptors in TNBS colitis. Inflamm Bowel Dis. 2005 Jun;11(6):533–40.

121. Martín a R, Villegas I, Alarcón de la Lastra C. The COX-2 inhibitor, rofecoxib, ameliorates dextran sulphate sodium induced colitis in mice. Inflamm Res. 2005 Apr;54(4):145–51.

122. Mitchell JA, Warner TD. COX isoforms in the cardiovascular system: understanding the activities of non-steroidal anti-inflammatory drugs. Nat Rev Drug Discov. 2006 Jan;5(1):75–86.

123. Singh VP, Patil CS, Jain NK, Kulkarni SK. Aggravation of inflammatory bowel disease by cyclooxygenase-2 inhibitors in rats. Pharmacology. 2004 Oct;72(2):77–84.

124. Morteau O, Morham SG, Sellon R, Dieleman L a, Langenbach R, Smithies O, et al. Impaired mucosal defense to acute colonic injury in mice lacking

cyclooxygenase-1 or cyclooxygenase-2. J Clin Invest. 2000 Feb;105(4):469–78.

125. Wan MX, Liu Q, Wang Y, Thorlacius H. Protective effect of low molecular weight heparin on experimental colitis: role of neutrophil recruitment and TNF-alpha production. Inflamm Res. 2002 Apr;51(4):182–7.

126. Wang K, Han G, Dou Y, Wang Y, Liu G, Wang R, et al. Opposite role of tumor necrosis factor receptors in dextran sulfate sodium-induced colitis in mice. PLoS One. 2012 Jan;7(12):e52924.

127. Holtmann MH, Douni E, Schutz M, Zeller G, Mudter J, Lehr H-A, et al. Tumor necrosis factor-receptor 2 is up-regulated on lamina propria T cells in Crohn's disease and promotes experimental colitis in vivo. Eur J Immunol. 2002 Nov;32(11):3142–51.

128. Mizoguchi E, Mizoguchi A, Takedatsu H, Cario E, de Jong YP, Ooi CJ, et al. Role of tumor necrosis factor receptor 2 (TNFR2) in colonic epithelial hyperplasia and chronic intestinal inflammation in mice. Gastroenterology. 2002 Jan;122(1):134–44.

129. Kwon KH, Murakami A, Hayashi R, Ohigashi H. Interleukin-1beta targets interleukin-6 in progressing dextran sulfate sodium-induced experimental colitis. Biochem Biophys Res Commun. 2005 Nov;337(2):647–54.

130. Arai Y, Takanashi H, Kitagawa H, Okayasu I. Involvement of interleukin-1 in the development of ulcerative colitis induced by dextran sulfate sodium in mice. Cytokine. 1998 Nov;10(11):890–6.

131. Neurath MF, Fuss I, Kelsall BL, Stuber E, Strober W. Antibodies to interleukin 12 abrogate established experimental colitis in mice. J Exp Med. 1995 Nov;182(5):1281–90.

132. Naito Y, Takagi T, Handa O, Ishikawa T, Nakagawa S, Yamaguchi T, et al. Enhanced intestinal inflammation induced by dextran sulfate sodium in tumor necrosis factor-alpha deficient mice. J Gastroenterol Hepatol. 2003 May;18(5):560–9.

133. Rothe J, Lesslauer W, Lotscher H, Lang Y, Koebel P, Kontgen F, et al. Mice lacking the tumour necrosis factor receptor 1 are resistant to TNF-mediated toxicity but highly susceptible to infection by Listeria monocytogenes. Nature. 1993 Aug;364(6440):798–802.

134. Loetscher H, Gentz R, Zulauf M, Lustig A, Tabuchi H, Schlaeger EJ, et al. Recombinant 55-kDa tumor necrosis factor (TNF) receptor. Stoichiometry of binding to TNF alpha and TNF beta and inhibition of TNF activity. J Biol Chem. 1991 Sep;266(27):18324–9.

135. Yamamoto T, Sekine Y, Kashima K, Kubota A, Sato N, Aoki N, et al. The nuclear isoform of protein-tyrosine phosphatase TC-PTP regulates interleukin-6-mediated signaling pathway through STAT3 dephosphorylation. Biochem Biophys Res Commun. 2002 Oct;297(4):811–7.

136. Dann SM, Spehlmann ME, Hammond DC, Iimura M, Hase K, Choi LJ, et al. IL-6 dependent mucosal protection prevents establishment of a microbial niche for attaching /effacing lesion-forming enteric bacterial pathogens. J Immunol. 2008 May;180(10):6816-26.

137. Burdelya L, Kujawski M, Niu G, Zhong B, Wang T, Zhang S, et al. Stat3 activity in melanoma cells affects migration of immune effector cells and nitric oxide-mediated antitumor effects. J Immunol. 2005 Apr;174(7):3925–31.

138. Atreya R, Neurath MF. Involvement of IL-6 in the pathogenesis of inflammatory bowel disease and colon cancer. Clin Rev Allergy Immunol. 2005 Jun;28(3):187–96.

139. Nishihara M, Ogura H, Ueda N, Tsuruoka M, Kitabayashi C, Tsuji F, et al. IL-6-gp130-STAT3 in T cells directs the development of IL-17+ Th with a minimum effect on that of Treg in the steady state. Int Immunol. 2007 Jun;19(6):695–702.

140. Horino J, Fujimoto M, Terabe F, Serada S, Takahashi T, Soma Y, et al. Suppressor of cytokine signaling-1 ameliorates dextran sulfate sodium-induced colitis in mice. Int Immunol. 2008 Jun;20(6):753–62.

141. Mahida YR, Kurlac L, Gallagher A, Hawkey CJ. High circulating concentrations of interleukin-6 in active Crohn's disease but not ulcerative colitis. Gut. 1991 Dec;32(12):1531–4.

142. Weber B, Saurer L, Mueller C. Intestinal macrophages: differentiation and involvement in intestinal immunopathologies. Semin Immunopathol. 2009 Jul;31(2):171–84.

143. Takada Y, Hisamatsu T, Kamada N, Kitazume MT, Honda H, Oshima Y, et al. Monocyte chemoattractant protein-1 contributes to gut homeostasis and intestinal inflammation by composition of IL-10-producing regulatory macrophage subset. J Immunol. 2010 Mar;184(5):2671–6.

144. Damiani CR, Benetton C a F, Stoffel C, Bardini KC, Cardoso VH, Di Giunta G, et al. Oxidative stress and metabolism in animal model of colitis induced by dextran sulfate sodium. J Gastroenterol Hepatol. 2007 Nov;22(11):1846–51.

145. Rugtveit J, Nilsen EM, Bakka A, Carlsen H, Brandtzaeg P, Scott H. Cytokine profiles differ in newly recruited and resident subsets of mucosal macrophages from inflammatory bowel disease. Gastroenterology. 1997 May;112(5):1493–505.

146. Ghia J-E, Galeazzi F, Ford DC, Hogaboam CM, Vallance B a, Collins S. Role of M-CSF-dependent macrophages in colitis is driven by the nature of

the inflammatory stimulus. Am J Physiol Gastrointest Liver Physiol. 2008 Mar;294(3):G770–7.

147. Stevceva L, Pavli P, Husband AJ, Doe WF. The inflammatory infiltrate in the acute stage of the dextran sulphate sodium induced colitis: B cell response differs depending on the percentage of DSS used to induce it. BMC Clin Pathol. 2001 Jan;1(1):3.

148. Kargl J, Andersen L, Hasenöhrl C, Stancic A, Fauland A, Magnes C, El-Heliebi A, Lax S, Uranitsch S, Haybaeck J, Heinemann A, Schicho R. GPR55 promotes migration and adhesion of colon cancer cells indicating a role in metastasis.Br J Pharmacol. Manuscript submitted for publication.

149. Hayakawa K, Mishima K, Nozako M, Hazekawa M, Irie K, Fujioka M, et al. Delayed treatment with cannabidiol has a cerebroprotective action via a cannabinoid receptor-independent myeloperoxidase-inhibiting mechanism. J Neurochem. 2007 Sep;102(5):1488–96.

150. Qualls JE, Kaplan AM, van Rooijen N, Cohen DA. Suppression of experimental colitis by intestinal mononuclear phagocytes. J Leukoc Biol. 2006 Oct;80(4):802–15.

151. Izzo RS, Witkon K, Chen AI, Hadjiyane C, Weinstein MI, Pellecchia C. Interleukin-8 and neutrophil markers in colonic mucosa from patients with ulcerative colitis. Am J Gastroenterol. 1992 Oct;87(10):1447–52.

152. Hans W, Scholmerich J, Gross V, Falk W. Interleukin-12 induced interferon-gamma increases inflammation in acute dextran sulfate sodium induced colitis in mice. Eur Cytokine Netw. 2000 Mar;11(1):67–74.

153. Cominelli F, Nast CC, Clark BD, Schindler R, Lierena R, Eysselein VE, et al. Interleukin 1 (IL-1) gene expression, synthesis, and effect of specific IL-1 receptor blockade in rabbit immune complex colitis. J Clin Invest. 1990 Sep;86(3):972–80.

154. Harris RE. Cyclooxygenase-2 (cox-2) blockade in the chemoprevention of cancers of the colon, breast, prostate, and lung. Inflammopharmacology. 2009 Apr;17(2):55–67.

155. Roberts PJ, Morgan K, Miller R, Hunter JO, Middleton SJ. Neuronal COX-2 expression in human myenteric plexus in active inflammatory bowel disease. Gut. 2001 Apr;48(4):468–72.

156. Feagins LA, Cryer BL. Do non-steroidal anti-inflammatory drugs cause exacerbations of inflammatory bowel disease? Dig Dis Sci. 2010 Feb;55(2):226–32.

157. Clapper ML, Cooper HS, Chang W-CL. Dextran sulfate sodium-induced colitis-associated neoplasia: a promising model for the development of chemopreventive interventions. Acta Pharmacol Sin. 2007 Sep;28(9):1450–9.

158. Wang D, Wang H, Ning W, Backlund MG, Dey SK, DuBois RN. Loss of cannabinoid receptor 1 accelerates intestinal tumor growth. Cancer Res. 2008 Aug;68(15):6468–76.

159. Sun H, Jiang L, Luo X, Jin W, He Q, An J, et al. Potential tumor-suppressive role of monoglyceride lipase in human colorectal cancer. Oncogene. 2013 Jan;32(2):234–41.

160. Nomura DK, Lombardi DP, Chang JW, Niessen S, Ward AM, Long JZ, et al. Monoacylglycerol lipase exerts dual control over endocannabinoid and fatty acid pathways to support prostate cancer. Chem Biol. 2011 Jul;18(7):846–56.

161. Kinsey SG, Nomura DK, O'Neal ST, Long JZ, Mahadevan A, Cravatt BF, et al. Inhibition of monoacylglycerol lipase attenuates nonsteroidal anti-inflammatory drug-induced gastric hemorrhages in mice. J Pharmacol Exp Ther. 2011 Sep;338(3):795–802.

162. Du H, Chen X, Zhang J, Chen C. Inhibition of COX-2 expression by endocannabinoid 2-arachidonoylglycerol is mediated via PPAR-γ. Br J Pharmacol. 2011 Aug;163(7):1533–49.

163. Endsley MP, Aggarwal N, Isbell MA, Wheelock CE, Hammock BD, Falck JR, et al. Diverse roles of 2-arachidonoylglycerol in invasion of prostate carcinoma cells: Location, hydrolysis and 12-lipoxygenase metabolism. Int J Cancer. 2007 Sep;121(5):984–91.

164. Klein TW. Cannabinoid-based drugs as anti-inflammatory therapeutics. Nat Rev Immunol. 2005;5(5):400–11.